Published in final edited form as:
Neuroscience. 2009 August 18; 162(2): 501–524. doi:10.1016/j.neuroscience.2009.05.005.

Multiple forebrain systems converge on motor neurons innervating the thyroarytenoid muscle

Douglas J. Van Daele and
Department of Otolaryngology-Head and Neck Surgery, University of Iowa

Martin D. Cassell
Department of Anatomy and Cell Biology, University of Iowa

Abstract

The present study investigated the central connections of motor neurons innervating the thyroarytenoid laryngeal muscle that is active in swallowing, respiration and vocalization. In both intact and sympathectomized rats, the pseudorabies virus (PRV) was inoculated into the muscle. After initial infection of laryngomotor neurons in the ipsilateral loose division of the nucleus ambiguous (NA) by 3 days post-inoculation., PRV spread to the ipsilateral compact portion of the NA, the central and intermediate divisions of the nucleus tractus solitarii (NTS), the Botzinger complex, and the parvocellular reticular formation by 4 days. Infection was subsequently expanded to include the ipsilateral granular and dysgranular parietal insular cortex, the ipsilateral medial division of the central nucleus of the amygdala, the lateral, paraventricular, ventrolateral and medial preoptic nuclei of the hypothalamus (generally bilaterally), the lateral periaqueductal gray, the A7 and oral and caudal pontine nuclei. At the latest time points sampled post-inoculation (5 days), infected neurons were identified in the ipsilateral agranular insular cortex, the caudal parietal insular cortex, the anterior cingulate cortex, and the contralateral motor cortex. In the amygdala, infection had spread to the lateral central nucleus and the parvocellular portion of the basolateral nucleus. Hypothalamic infection was largely characterized by an increase in the number of infected cells in earlier infected regions though the posterior, dorsomedial, tuberomammillary and mammillary nuclei contained infected cells. Comparison with previous connectional data suggest PRV followed three interconnected systems originating in the forebrain; a bilateral system including the ventral anterior cingulate cortex, periaqueductal gray and ventral respiratory group; an ipsilateral system involving the parietal insular cortex, central nucleus of the amygdala and parvicellular reticular formation, and a minor contralateral system originating in motor cortex. Hypothalamic innervation involved several functionally specific nuclei. Overall, the data imply complex central nervous system control over the multi-functional thyroarytenoid muscle.[297 words]

Keywords

larynx; voice; motor control; amygdala; insula; medulla

Corresponding Author: Douglas J. Van Daele, M.D., Department of Otolaryngology – Head and Neck Surgery, Roy J and Lucille A Carver College of Medicine, University of Iowa, 21265PFP, 200 Hawkins Drive, Iowa City, IA 52242, Phone: (319)353-8162, FAX: (319)356-4547, EMAIL: douglas-van-daele@uiowa.edu.

Introduction

The principal function of the larynx is to control and modulate the flow and pressure of air entering and leaving the lungs and lower airway. Within the larynx the glottis, consisting of the plicae vocales (vocal folds) and the gap between them, the rima glottidis is the primary area of control. Airflow must be regulated differently during respiration, coughing, swallowing, and vocalization. The glottis completely closes in some situations, e.g. swallowing, coughing, while in others the position and tension of the vocal folds in others in others, e.g. vocalization. The general consensus is that this broad range of functional requirements is effected by complex interactions between groups of neurons in the medulla that act as pattern generators each dedicated to controlling laryngeal muscle action for a particular action, e.g. swallowing (Jean, 1984; Jean, 2001). These pattern generators ultimately exert close control over laryngeal motorneurons but in addition provide an interface through which numbers of central systems can influence laryngeal function.

Electromyographic studies in a number of species (Ertekin and Palmer, 2000; Perlman et al., 1999; Sasaki and Suzuki, 1976) indicate that all intrinsic and extrinsic muscles of the larynx are engaged at some point during the complex behaviors involving the glottis, though some muscles show little activity in some functions (Ludlow, 2005; Poletto et al., 2004) However, the thyroarytenoid muscle (TA), which is located within the bulk of the vocal folds, appears to be active in swallowing, vocalization, normal respiration and coughing (McCulloch et al., 1996; Perlman et al., 1999). This suggests that the motor neurons in the nucleus ambiguus (NA) innervating the TA must be directly connected to the various pattern generators dedicated to these functions.

Direct and indirect connections linking cortical areas with laryngeal motor neurons have been postulated and laryngeal representation in the motor cortex has been well-established in primates, including man (e.g. Hast et al., 1974; Jurgens, 1976; Simonyan and Jurgens, 2002; 2005; Jurgens and Ehrenreich, 2007;Brown et al., 2007). However, imaging studies of co-ordinated functions such as swallowing and sound/speech production (e.g. Martin et al., 2004; Lowell et al., 2008; Ackermann and Rieker, 2005) show activation of areas outside the motor cortex, most notably the insula. Additional limbic areas such as the anterior cingulate cortex (Jurgens, 1976) and amygdala have been implicated in control of laryngeal function. How these limbic cortical areas are connected with laryngeal motor neurons remains largely unknown.

TA motor neurons in the rat are located in the caudally-situated loose portion of the NA along with motorneurons innervating the other intrinsic laryngeal muscles with the exception of cricothyroid (Bieger and Hopkins, 1987; Lobera et al., 1981; Portillo and Pasaro, 1988). Conventional anatomical tracing studies that have examined the connections of the NA have not examined the specific innervation of TA motor neurons though there are studies addressing connections of the NA as a whole with areas containing specific pattern generators (Nunez-Abades et al., 1990) and with specific forebrain areas (ter Horst et al., 1984). A central problem with studies involving injection of tracers into the NA is that it is nearly impossible to prevent tracers from diffusing into adjacent reticular areas which may have different connections from the NA itself (ter Horst et al., 1984). Similarly, inclusion in injection sites of preganglionic parasympathetic neurons in the ventrally-situated external NA makes conclusions about the connections of motor neurons with hypothalamic and forebrain areas difficult to obtain.

The present study was designed principally to i) determine the connectivity of the motor neurons innervating the thyroarytenoid muscle with patterns generators in the pons and medulla and ii) determine which hypothalamic and forebrain areas are indirectly connected with these motor neurons. To this end, we have used injections of the transneuronally spreading pseudorabies virus (PRV) into the TA in sympathectomized and intact rats. We then followed

the course of infection of successive levels of the CNS for up to five days to determine which systems have convergent input to TA motor neurons and at what level these various systems may interact. Parts of this work have appeared in Abstract form (Van Daele and Cassell, 2007; Van Daele and Cassell, 2006).

EXPERIMENTAL PROCEDURES

Experiments were performed on a total of 45 adult male Sprague-Dawley rats (wt approximately 275 gm). All procedures were consistent with the NIH and Society for Neuroscience guidelines and were approved by the institutional Animal Care and Use Committee. All surgical procedures were carried out under sterile conditions and under ketamine (40mg/kg) with xylazine (5 mg/kg) intraperitoneal anesthesia. Bupivacaine (5%) was applied topically to the wound to reduce pain.

Injections of the attenuated Bartha strain of pseudorabies virus labeled with green fluorescent protein (GFP, kindly provided by Lyn Enquist, Princeton, NJ) were made as a single bolus of 10 microliters at 6×10^{23} pfu directly into the thyroarytenoid muscle(Smith et al., 2000). The larynx was exposed by a midline skin incision and the cricothyroid membrane identified (Bauman, et al., 1999). Aliquots of virus were thawed from − 80 degrees Celsius and vortexed prior to injection. No aliquot underwent a freeze-thaw cycle more than three times. The needle of a beveled Hamilton microsyringe was inserted though the membrane a distance of 2 mm and the injection made. Identification of the injection site was difficult because PRV was rapidly cleared from the TA thus the PRV solution was mixed with 2% choleratoxin B fragment-horseradish peroxidase (HRP) in some injections to allow detection of the injectate through peroxidase histochemistry. After the injection, the skin wound was sutured and the animals allowed to recover.

Eight animals were sympathectomized by removal of the superior cervical ganglion at the time of injection. Successful elimination of cranial sympathetic innervation was confirmed by the presence of ptosis. Control experiments consisted of unilateral sectioning of the superior (two animals) and recurrent laryngeal nerves (three animals), and unilateral removal of the superior cervical ganglion *and* sectioning of the cervical vagus at the base of the skull (three animals) at the time of injection. Additionally, four animals received the usual volume of injectate sprayed onto the mucosa covering the vocal folds. This was accomplished by pushing the syringe needle through the thyrohyoid membrane into the supraglottic space.

In addition, to confirm that only TA motorneurons were being infected initially, four animals were given PRV-GFP inoculations into the TA muscle and at the same time a PRV strain with a Lac-Z reporter was injected into the ipsilateral posterior cricoarytenoid (PCA) muscle (three cases) or cricothyroid (one case). In contrast to TA, the PCA is an abductor of the vocal folds while the cricothyroid (CT) influences glottic position by tilting the thyroid cartilage on the cricoid cartilage.

Signs of viral infection (ruffled fur, shaking, lethargy) generally did not appear before 72 hours post-inoculation. Groups of animals were euthanized at 2, 3, 4 and 5 days after PRV injection by intraperitoneal injection of pentobarbital (100mg/kg). Following cessation of respiration, the thorax was opened and blood flushed out with 100 ml of physiological saline injected through the left ventricle. This was followed by 500ml of ice-cold fixative consisting of 4% paraformaldehyde in phosphate buffered saline (pH7.3). After thirty minutes of fixative perfusion, the cranium was opened and the side of the brain contralateral to the injection marked with a notch. Brains and larynges were then removed and post-fixed for 24 hours in the fixative then placed in 30% dextrose prior to sectioning. Frozen sections of the brain 30–50 microns thick were cut in the horizontal or coronal plane; transverse sections of the larynx were also

cut frozen at 50 microns (μM)thick. In four animals euthanized at 2 and 3 days post-inoculation, the nodose ganglia were removed on both sides and frozen sections cut longitudinally at 50μM thickness.

Viral infection of neurons was detected through immunocytochemical labeling of the green fluorescent protein or Lac-Z. Brain sections were incubated in the particular antibody (anti-GFP; Vector Labs; #BA-0702 at a dilution ratio of 1:1000 or biotinylated anti-Lac-Z, Sigma-Aldrich, #G4644 at a dilution ratio of 1:1000) for 24–48 hours at 4 degrees Celsius. Following incubation in a biotinylated secondary antibody, final staining was done using avidin-horseradish peroxidase reagents (Vector Elite ABC kits) and 0.01% 3,3′-diaminobenzidine (DAB)in 2% aqueous nickel ammonium sulfate. Sections were washed and mounted in serial order on slides, dried, dehydrated and cleared and permanently mounted in Permount. Selected slides were counterstained with cresyl violet. In some cases, following immuno-detection of PRV, sections were re-incubated in either anti-parvalbumin (PVAB, Swant, Switzerland; 1:1000 dilution), anti-calcitonin gene-related peptide (CGRP, CalBiochem #PC205L, 1:10,000 dilution) or anti-choline acetlytransferase (ChAT, Boehringer Mannheim; 1:1000 dilution) overnight. Sections were then incubated in biotinylated secondary antibodies and final staining done using avidin-HRP reagents (Vector Elite ABC kits) and 0.01% 3,3′-diaminobenzidine (DAB). This gave a brown color to PVAB, CGRP and ChAT immunoreactive elements in contrast to the blue-black staining of PRV-GFP infected cells.

For double labeling in the four animals with TA and PCA injections, GFP immunolabeling was performed on alternate sections first using DAB plus nickel ammonium sulfate as chromagen. After extensive washing, one-half of these sections plus the alternate sections were re-incubated in the anti-Lac-Z antibody overnight: DAB without nickel ammonium sulfate was used as chromagen. In these preparations, PRV-GFP infected cells were grayish-black with punctate black particles in the perikarya and dendrites while PRV-Lac-Z infected cells had an amorphous light brown appearance. Double-labeled cells were identified as such by the presence of black particles in cells stained brown and double-staining confirmed by using either a deep yellow filter to attenuate the brown staining or examination of the adjacent sections stained for just PRV-GFP. In addition, a sample of sections from two PCA injection cases were immunostained for Lac-Z using a rhodamine-conjugated secondary antibody and examined under epifluorescence.

Sections of the larynx were mounted onto slides directly after cutting but kept moist by storage in a humidity chamber. Where CTB-HRP had been injected, selected slides were first immersed in 0.01M acetate buffer (pH3.3) for 1–2 minutes followed by incubation for 10–20 minutes in a medium containing acetate buffer, 0.001% 3,3′ tetramethylbenzidine, 1% sodium nitroprusside and 0.03% hydrogen peroxide. Peroxidase activity was identified by the presence of dense blue crystals. Selected laryngeal sections were counterstained with neutral red or hematoxylin and eosin, mounted and cover-slipped.

Sections were examined with a Nikon Labophot equipped with 8.0 megapixel digital camera. For each case, every section was examined under 10X magnification and the distribution of labeled neurons and the outlines of major brain structures plotted digitally for every fourth section. Identification of structures was done on the basis of cytoarchitectural or immuno-staining characteristics and through comparison with a large set of reference sections and the atlases of Paxinos and Watson (2005) and Swanson (Swanson and Swanson, 2004). Terminology reflects that employed by Paxinos and Watson except where primary references have been used. All digital photomicrographs were processed using Adobe Photoshop version 7.0. No artificial enhancements were made during processing though several pictures were digitally retouched to remove dust spots and other blemishes: none of this affected image data.

For quantification of infected cells in the nucleus ambiguus (NA) and nucleus tractus solitarii (NTS), two sampling and counting methods were employed. For the NA bilaterally, GFP-immunoreactive cell fragments were counted on *every* section (between 9 and 15 50 μM thick horizontal sections) through the nucleus. Digital images (450X final magnification) of the NA were made and overlain to identify fragments of the same cell appearing on more than one section: only the largest fragment in one section was counted. The numbers thus represented an estimate of the *total number of infected cells* and no corrections needed to be applied. For the NTS, a single (horizontal) section containing roughly the dorsoventral mid-plane of the NTS was selected from a sample of cases from each time point (four early 4 day; four late 4 day; four early 5 day and two late 5 day) and control experiment (two superior laryngeal nerve section; three recurrent laryngeal nerve section; three vagus nerve section). The selected section, identical in level for all cases, was chosen as it contained the medial, central, interstitial, intermediate and commissural divisions of the NTS, and a portion of the area postrema (AP). In each subdivision on both sides, the number of GFP-immunoreactive cell fragments in excess of 10μM in diameter was counted. This diameter was selected to eliminate counting GFP-immunoreactive glia. Data are presented (Table 2) as *(uncorrected) fragment counts*.

RESULTS

i) Virus injection into thyroarytenoid muscle

The thyroarytenoid muscle in the rat consists of two components, medial and lateral, that run parallel to each other between the thyroid and arytenoid cartilages (Inagi et al., 1998). The medial component runs from the vocal process of the arytenoid cartilage and is thought homologous to the vocalis muscle of humans. In most of the larynges examined, the viral injection sites appear to involve both components of TA at roughly their mid-points (Fig. 1A and B). GFP fluorescence was detectable in larynges from animals euthanized at 2 and 3 days post-inoculation but after this immunocytochemical staining for GFP generally did not result in labeling of the muscle itself though numerous immunopositive polymorphonuclear lymphocytes and fibroblasts were seen around the needle track in the muscle. Thus the lack of muscle staining may be due to clearance of virus. No immunolabelling was seen in any other laryngeal muscle nor in the adipose and glandular tissue located between the TA and the thyroid cartilage (Fig. 1A).

In the nodose ganglia removed from four animals euthanized at 2 and 3 days post-inoculation, GFP labeling in neurons was observed in only one (ipsilateral) specimen and then only in two neurons (Fig. 1C).

ii)Viral labeling in the brain

A total of 25 animals out of 29 (non-control) receiving intralaryngeal injections showed uptake of virus from the TA injection and infection of neurons in the brain (Table 1). Substantial differences in the number and location of infected neurons were evident in brains sampled at the three different time points, and in the vagus and laryngeal nerve sectioned animals and those with mucosal viral sprays. However, there were only modest differences in overall distribution pattern between sympathectomized and non-sympathectomized animals. These differences primarily related to the numbers of infected neurons in the reticular formation, the perifornical hypothalamic region, the infralimbic cortex and the area postrema and subfornical organ which were generally only present in the non-sympathectomized animals. The initial pattern of infection in the NA (Fig. 1D;2A–D), nucleus tractus solitarius (Fig. 4A–D) and other ponto-medullary structures was remarkably similar in sympathectomized and non-sympathectomized animals.

Within the 4 and 5 day survival groups there were also substantial differences in extent and pattern of labeling. However, these patterns fell into two distinct groups for each day and are described below as the *early* and *late* patterns for days 4 and 5.

a)3 day animals—In **7** of the 10 animals (all non-sympathectomized) sacrificed at 2 and 3 days post-inoculation (p.i.), no viral labeling was detected in the brain. Since all cases sacrificed at 4 and 5 days had CNS infection, it would appear viral labeling from TA injection first appears in the brain 60–72 hours post-inoculation. In the remaining three cases, a few moderately immunostained neurons were found in the nucleus ambiguus (NA) and the intermediate division of the NTS on the same side (ipsilateral). In all three cases, infected cells were seen in the rostral part of the loose (NAl) division of the NA (Fig. 1D); no infected cells were identified in the compact NA (NAc).

b) 4 day animals—Eight animals (three sympathectomized) sacrificed at 4 days p.i. showed infection of the brain of which one had an infection pattern almost identical to that seen in animals sacrificed at 3 days p.i.; three animals had more infected neurons in the NA (Fig. 2A and B) and more regions with infected neurons than 3 day animals but with infection restricted to the hypothalamus, midbrain pons and medulla (early day 4). Four animals had a still more advanced pattern of labeling with infected cells in the amygdala, cortex and hypothalamus (late day 4).

All four cases with combined TA and PCA injections exhibited the late day 4 pattern of infection and numbers of infected neurons were comparable to those found after single muscle injections. Few double-infected neurons were identified and the general appearance was of adjacent or mixed but separate populations of neurons (Fig. 2C and D). In the nucleus ambiguus, neurons infected from the PCA were more rostrally located in the loose part than TA neurons and there were numbers of PCA neurons in the semi-compact portion. In all cases, infected neurons were present in the NAc, though their number varied. In the case illustrated, roughly equal numbers of large, single-labeled neurons were mixed in the dorsolateral part of the NAc. In this case, several small, double-labeled neurons were observed in the reticular formation adjacent to the NA (Fig. 2C and D).

Early pattern(Table 1): this pattern, found in three animals euthanized at 4 days and two at 5 days (see below), represents a progression over the typical three day pattern, and is consistent with transneuronal infection of second order neurons. In the medulla, infected neurons were found in the ipsilateral loose part of the NA, as seen in 3 day animals, but unlike those cases a number of infected cells were found in the ipsilateral compact NA, in all cases located along the dorsomedial part of NAc (Fig. 2A; Table 2). The more ventrally and laterally placed group of motor-neurons innervating the cricothyroid muscle (Bieger and Hopkins, 1987) did not contain immunolabled neurons (Fig. 3A). A conspicuous feature of the infected cells in the NAc was the “bundling” of immunolabeled dendrites parallel to the rostrocaudal axis of the NA (Fig. 2B) (Altschuler et al., 1991). In one case, a few infected neurons were seen caudally near the spinomedullary junction in the region usually referred to as the ventral respiratory group (VRG) or nucleus retroambigualis (NRA) (Fig. 3A). Infected cells were now consistently seen in the reticular formation dorsal and ventral to the NA, and predominantly ipsilaterally. The parvicellular reticular formation (PCRT) located immediately dorsal and ventral to the NA contained a sparse, loosely distributed population of infected cells (Fig. 3A), and occasional (1–3) cells were seen in the ipsilateral lateral and dorsal gigantocellular reticular areas, and in the area just lateral to the hypoglossal nucleus (Probst’s nucleus [Prb]).

Ventral to the NA, infected cells were seen just caudal to the facial nucleus in the region termed the Bötzinger complex (Alheid et al., 2002; Fig. 3C). In a case sectioned sagittally (Fig. 3A), immunolabelled cells could be seen clustered up against the facial nucleus but separated from

a scattered caudally situated group by an unlabeled area that appeared to correspond to the pre-Bötzinger region. A few infected cells were identifiable in the lateral reticular and lateral paragigantocellularis regions.

Dorsally, the ipsilateral central subdivision of the NTS contained infected cells (Fig. 3B; Table 2), and in both sympathectomized cases, infected cells were found ipsilaterally in the intermediate and interstitial NTS subdivisions and in the area postrema (Fig. 4A;Table 2). The infected cells in the NTS were arranged in small clusters that co-extended in a line parallel to the tractus from about 50μM to 1200μM anterior to the obex. Notably, each cluster appeared embedded in a patch of immunostained neuropil (Fig. 4A).

Ascending progression of infection was indicated by small numbers of infected neurons being present (bilaterally with ipsilateral predominance) in the A7 and subceruleus regions of the rostral pons, the mesencephalic trigeminal nucleus, locus ceruleus, dorsal raphe, lateral and ventrolateral periaqueductal gray (PAG) and in the non-sympathectomized animals the perifornical area of the hypothalamus.

Late pattern (Table 1): One sympathectomized and three non-sympathectomized animals sacrificed at 4 days p.i. and five animals euthanized at 5 days showed a more advanced pattern of infection with more contralateral structures containing immunolabled neurons (though the overall infection was much greater ipsilaterally) and spread of infection to cells in the telencephalon. As in earlier cases, large neurons in the ipsilateral NAc, NAsc and NAl were infected in a similar pattern (Table 2). Contralaterally, neurons were infected in the NAc and NAl but many of these were not the large motor neurons but smaller fusiform cells. The numbers of infected cells in the ipsilateral PCRT (Fig. 5A) and A7/subceruleus region was greatly increased over that seen in early 4 day p.i. animals, and in addition, infected cells were seen in the dorsal intermediate reticular formation (IRT) and in the alpha subregion of the PCRT (PCRTa) caudal to the descending limb of the facial nerve.

Ventral to the NA, there was increased numbers of infected cells in the Bötzinger complex and the rostral ventral respiratory group as well as the presence of occasional infected cells ventral to the facial nucleus in the region of the retrotrapezoid nucleus. Double immuno-staining with an antibody to parvalbumin revealed PRV infected cells mixed with parvalbumin immunopositive cells in the Bötzinger complex and VRG (Alheid et al., 2002; Figs.3D, E). However, the pre-Bötzinger region, which lacks parvalbumin immunopositive cells, contained very few infected cells (Fig. 3C). A small increase in the numbers of cells in the lateral paragigantocellularis region over early day 4 cases was observed.

Infection in the ipsilateral NTS was modestly increased over earlier time points and was still largely confined to the central, intermediate and interstitial subdivisions (Figs.3B;5A; Table 2) though infected cells were seen now in the contralateral cNTS, the commissural NTS, and in the area subjacent to the rostromedial (gustatory) portion of the NTS (Fig. 4B). The area postrema was also labeled in non-sympathectomized cases. In the pons and midbrain, greater numbers of infected cells were identified in the locus ceruleus (Fig. 5B) and ventral periaqueductal gray but there were no new areas containing infected cells except in one non-sympathectomized case small numbers of infected cells were present bilaterally in the substantia nigra, pars reticulata.

The principal differences between early and late 4 day animals lay in the expansion of infected areas in the hypothalamus (Table 1) and the presence of infected neurons in the amygdala and cortex. In the hypothalamus, infected cells were now present in considerable numbers in the parvicellular paraventricular nucleus and medial and lateral preoptic areas bilaterally and in the ipsilateral lateral hypothalamic area along the inner edge of the medial forebrain bundle

(Figs.6; 7A and B). In the non-sympathectomized animals (Fig. 7A), there appeared to be more infected cells in the more lateral and posterior parts of the lateral hypothalamus. Immunolabelled cells in the amygdala were restricted to the medial division of the central nucleus and in both cases were clustered in its rostral part.

A modest number of infected cells were identified in all cases in the ipsilateral granular (gPA) and dysgranular (dPA) parietal insular cortex at the level of bregma (Fig. 8A). The cells were mostly located in layer V and formed a distinct cluster roughly 300 microns in diameter. Occasional, isolated, infected cells were seen in the dysgranular (dPI) and agranular posterior (aPI) insular cortex, the dysgranular anterior (dAI) insular cortex and the entorhinal cortex. In one non-sympathectomized case, a few cells were seen in the ipsilateral infralimbic area.

c)5 day animals (Table 1; Fig. 9)—All non-control animals killed 5 days after inoculation of PRV into TA showed infection of the CNS. Of these fourteen animals with infected neurons in the CNS, two had a pattern identical to the early 4 day one, five had distributions of infected neurons very similar to the late 4 day pattern, and seven had more extensive infections than seen at earlier time-points. Two of these animals had infected neurons in a number of cortical areas combined with evidence of viral clearance from the medulla; these will be described as the late day 5 pattern while the other five animals as early 5 day.

Early pattern (Fig. 8): All five cases showed extensive gliosis in the ipsilateral NA and a significant reduction in the numbers and intensity of immunostaining of large cells in the ipsilateral NAc and NAl (Table 2). On Nissl counterstained sections, weakly immunostained cells in the NA could be seen surrounded by glia and other large immunonegative cells also surrounded by glia showed loss of the intense basophilia characteristic of normal NA neurons (Fig. 2B). On the ipsilateral side, gliosis was evident in the NTS (Fig. 4C), PCRT and Probst's nucleus, where there appeared to be fewer and more weakly immunostained cells (for NTS, see Table 2) than in late 4 day pattern animals, though contralaterally, immunostaining was robust in both areas and many infected cells were present (Fig. 9). Infected cells were present bilaterally in the NTS and were concentrated in the central, commissural, intermediate and interstitial subdivisions (Table 2). Compared to the late 4 day pattern, more cells were present bilaterally in the region subjacent to the rostromedial NTS (Table 2). In all animals, the locus ceruleus was bilaterally infected and on alternating counterstained sections, every neuron there appeared to be infected. In the midbrain, the dorsal part of the ventrolateral column of the caudal PAG was filled with infected cells bilaterally and there was increased numbers of infected cells in the ventrolateral portion of the column, the dorsal and dorsolateral column PAG columns, and the pedunculopontine tegmentum on both sides (Fig. 5C). A cluster of neurons in the supraoculomotor PAG was seen in every case. Rostrally, there were many fewer cells in the PAG, mostly in the dorsolateral column ipsilaterally and ventrolateral column contralaterally (Fig. 5D). Ventrally, the caudomedial substantia nigra, pars compacta (A9) and retrorubral field (A8) contained numbers of infected cells bilaterally.

Increased numbers of infected cells were evident in the diencephalon. Most cells in the early infected areas of the hypothalamus (lateral hypothalamus, parvicellular paraventricular, lateral, medial and median preoptic areas) were immunopositive for PRV, and small numbers of infected cells were now present in the periventricular, dorsomedial, ventromedial, tuberomammillary and pre-mammillary nuclei. A few infected cells were now identifiable in the caudal thalamus in an around the posterior commissure and fasciculus retroflexus. In the non-sympathectomized animals, infected cells were also present in the subfornical organ and in the lateral septum, predominantly ipsilaterally.

The most dramatic difference with late 4 day cases in the distribution of infected neurons was in the telencephalon. The medial division of the central nucleus (CeM) on both sides contained

many infected cells (though with ipsilateral dominance) and ipsilaterally infection had spread to cells in the lateral division (CeL) and the substantia innominata (SI) and bed nucleus of the stria terminalis (BNST) (Fig. 10A and B). In one case a small number of infected cells was found in the posterior or parvicellular part of the basolateral amygdaloid nucleus. In two cases, a few immunolabeled cells were located in the core region of the ipsilateral nucleus accumbens. This pattern of infection was the same in sympathectomized and non-sympathectomized animals.

Cortical infection was much more extensive than found in the late 4 day pattern, both in terms of numbers of infected cells, and cortical regions infected (Fig. 8B; 11A and B). A substantial cluster of infected neurons was now present in the ipsilateral insular cortex extending from the level of bregma to roughly 0.5 mm behind with neurons being located in both layers II/III and V in the granular and dysgranular PA, and layers II and III in the adjacent agranular PA (Fig. 11B. Three new clusters of infected cells were now consistently present outside of this grouping: one in layers II and III of the dysgranular anterior insular cortex at about 2–2.5mm anterior to bregma; another in superficial layers of the posterior insular cortex roughly at the point where the middle cerebral artery crosses the rhinal sulcus; and a third in layer V of the granular and dysgranular PA at approximately 2.5mm behind bregma (Fig. 11B). Small clusters of infected neurons were also scattered throughout the agranular insular cortex up to 4 mm behind bregma (Fig. 11B). Noticeable in all three cases were occasional cells in the adjacent second somatosensory area (S2). Immunolabeled cells in both areas were mostly in layers 2 and 3. In the non-sympathectomized animals, layer V of the infralimbic cortex on both sides contained substantial numbers of infected neurons and more dorsally, on the ipsilateral side only, small numbers of neurons were present in layer V of the ventral anterior cingulate area. In three cases, a small patch of infected cells was found in layer 5 of the contralateral frontal cortex in an area corresponding to the face area of primary motor cortex.

Late pattern: The principal differences between the early 5 day pattern and the late one are: reduction in the number of infected cells in the pons and medulla ipsilaterally (Table 2); symmetrical bilateral infection of structures in the midbrain, hypothalamus and basal forebrain though with heavier immunolabeling contralaterally; further transneuronal spread of viral infection to motor and sensory cortices.

Infected cortical neurons were now present bilaterally in the granular, dysgranular and agranular posterior and parietal insular cortices in both cases. Infected cells were located in layers II–V in all these areas. In the medial frontal cortex, infection had now spread to include the adjacent prelimbic and ventral anterior cingulate areas with most neurons being present in layers II and III on both sides (Fig. 8C). Noticeably, infected cells were now present in substantial numbers in layer V along the upper dorsolateral portion of the frontal cortex in an area corresponding to the head region of motor cortex (M1) (Fig. 8D). The labelling was heaviest contralateral to the injection site though significant numbers of infected cells were present ipsilaterally. The first (S1) and second (S2) sensory cortices both contained infected cells on the *ipsilateral* side but the greatest number of infected cells was seen in contralateral S1 (Fig. 8D). The immunolabeled cells in both areas were confined to distinct patches in the head representation area.

Other areas containing infected neurons but not found in earlier cases include the anterior thalamic nuclear complex, the CA1 area of the hippocampus, and the dorsal tegmental nucleus in the midbrain.

d) Control Experiments—Four types of direct control experiments were performed: ipsilateral section of either the recurrent or superior laryngeal nerves; ipsilateral vagotomy and removal of the superior cervical ganglion; spraying PRV directly into the interior of the larynx.

i) Superior laryngeal nerve section: In both cases with unilateral section of the SLN sacrificed at 5 days p.i., the pattern of infection was virtually identical to a typical late day 4 pattern (Table 2). In the ipsilateral NA, infected neurons were present in all subdivisions. The pattern of labeling in NTS subdivisions was essentially the same as that found in late day 4 cases (Table 2).

ii) Recurrent laryngeal nerve section: Unilateral section of the RLN in the tracheoesophageal groove or the vagus below the branching of the SLN following PRV inoculation of the TA was performed in three animals. Two animals had CNS infections and resulting distributions of infected cells resembling early 4 day patterns (cases 2 and 3, Table 2) with the exception that infection was heaviest *contralateral* to the inoculation side. Neither of these two direct RLN section cases had infected cells in the NA on the inoculated (ipsilateral) or contralateral sides (Table 2). In these cases, infected cells were present in the contralateral PCRt and subceruleus/A7 region and in the intermediate and commissural NTS bilaterally though no immunolabeled cells in the NA on either side could be identified. Rostral to the midbrain, the only infected cells were in the contralateral perifornical area and ipsilateral medial preoptic area. The late day 4 pattern case (section of vagus below SLN – case 1, Table 2) presented a similar medullary pattern of infection except that the NA had many more infected neurons contralaterally and there was bilateral infection of the PCRt. In the diencephalon and forebrain, the perifornical area, paraventricular and lateral hypothalamus on both sides contained infected cells, and the medial central nucleus (CeM) was bilaterally infected, with a contralateral dominance. The contralateral dysgranular insular cortex contained infected cells in layers III and V.

iii) Vagotomy/sympathectomy: Section of the vagus nerve at the base of the skull combined with extirpation of the superior cervical ganglion was undertaken in three cases following PRV inoculation of the TA. In all cases, the subsequent pattern of infection was almost identical to that found after RLN section, viz. lack of infection of the ipsilateral NA though with numbers of infected neurons in contralateral structures (Table 2). In one case (case 2, Table 2), despite a predominantly contralateral early 5 day pattern of infection, the *ipsilateral* dysgranular insular cortex was infected whereas only a few immunolabeled cells were identified there contralaterally.

iv) No infection was detected in the brains of animals given viral sprays into the laryngeal mucosa.

DISCUSSION

The present study has mapped the transneuronal spread of PRV-GFP through the rat forebrain following inoculation of the virus into an intrinsic laryngeal muscle, the thyroarytenoid (TA). The overall distribution of infected neurons was remarkably consistent across animals and the progression of infected CNS structures was time-dependent and consistent with known first, second- and third-order connections of these infected regions. Sympathectomy greatly attenuated infection of a number of autonomic related structures but infection of several areas commonly associated with autonomic function, e.g the paraventricular hypothalamic nucleus, the central nucleus of the amygdala, the insula, was unchanged. Even at the latest time points (5 days post-inoculation) sampled, viral infection was not widespread and large areas of the CNS did not contain infected cells. These general observations support the contention that PRV spread through restricted but densely interconnected neural networks following initial infection of TA motorneurons in the nucleus ambiguus.

It is unlikely that any major brain structures within the networks ultimately influencing the TA muscle were uninfected. The restriction of second-order and subsequent transneuronal infection to neurons synaptically connected with the initially infected cells is largely dependent

on a glial reaction that cordons off free virus released from the infected cell body and dendrites (Card et al., 1993). In the present study, gliosis was first evident in the NA of animals sacrificed at day 4, notably around immunopositive cells and their dendrites and was present cells in second-order structures in the medulla and pons, such as the parvicellular reticular formation, by 5 days. Noticeable in some day 5 cases was the loss of immunostaining and chromatolysis in NA motor neurons surrounded by glia (Fig. 2B), possibly indicating death of infected NA cells by this point.

Specificity of inoculation

Thyroarytenoid is one of two laryngeal muscles (the other is lateral cricoarytenoid) that are wholly or almost completely located within the cartilaginous framework of the larynx (Fig. 1B). Unilateral inoculation of virus into the TA without contamination of other muscles thus posed no great problem. Injections were made through the cricothyroid membrane, thus avoiding the more caudally located cricothyroid and lateral cricoarytenoid muscles. Simultaneous injection of the TA and posterior cricoarytenoid muscle with differently tagged PRV (GFP and LacZ) led to two partially overlapping populations of infected neurons in the loose and semi-compact parts of the NA (Fig. 2C and D). A few double-labeled neurons were identifiable in the NAc and adjacent PCRT but most pontine and medullary structures (e.g. NTS, VRG, A7) showed single-labeled neurons only. Overall, these observations support the assumption that PRV transport to the CNS was solely from the innervation of the TA muscle.

Spread of virus via sympathetic fibers innervating vascular beds in muscles may result in labeling of central autonomic systems and unilateral/bilateral sympathectomy has been widely employed in viral tracing studies of craniofacial muscle efferents (e.g. Travers and Rinaman, 2002; Giaconi et al., 2006). Surprisingly, we found little or no infection in the upper (cervicothoracic) portion of the intermediolateral cell column in most of the non-sympathectomized animals and structures such as the A5 noradrenergic group, which are infected very early following PRV inoculation of sympathetic ganglia (Strack et al., 1989a; Strack et al., 1989b) or the adrenal medulla (Li et al., 1992), only ever contained a few infected neurons after long incubation times. Additionally, section of the vagus nerve or recurrent laryngeal nerve with the superior cervical ganglion intact abolished ipsilateral infection of the medulla. However, sympathectomy clearly reduced or abolished infection of the perifornical hypothalamus, infralimbic cortex, the circumventricular organs (the subfornical organ and area postrema), and the ventral raphe, consistent with other studies (e.g. Ter Horst et al., 1996). Additionally, subtle changes in the numbers of infected cells in the parvicellular and lateral reticular formation and lateral hypothalamus were consistently observed. PRV transport via the sympathetic innervation of intrinsic laryngeal structures, albeit minor, was thus a confounding factor in the transneuronal labeling in non-sympathectomized animals.

The only other possible laryngeal sites of viral uptake are the secretomotor parasympathetic fibers innervating the large mucous glands located lateral to the TA muscle and/or postganglionic sympathetic fibers innervating glands and vascular structures. In no case was GFP-immunolabeling or macrophage infiltration seen in the intralaryngeal mucous glands though in several cases a few (3–8) small diameter cells in the external formation of the NA were seen to be infected. The external NA contains pre-ganglionic parasympathetic neurons sending axons mainly to cardiothoracic viscera (Standish et al., 1995; Ter Horst et al., 1996). The location of pre-ganglionic neurons providing input to post-ganglionic secretomotor fibers destined for the larynx is unknown so the possibility that some component of the observed pattern of infection was derived from transneuronal spread of PRV from these neurons cannot be entirely eliminated.

The possibility of uptake from parasympathetic nerves innervating upper respiratory structures other than the larynx must be considered. Jansen and colleagues (Jansen et al., 1993) reported

transneuronal PRV infection of a number of structures found infected here (e.g. central amygdaloid nucleus, lateral and perifornical hypothalamus) after PRV inoculation of the submandibular salivary gland. The labeling of telencephalic and diencephalic structures was thought to be second-order labeling subsequent to PRV infection of the superior salivatory nucleus. Infection of a few neurons in the superior salivatory nucleus was seen in two late day five cases only, both of which had extensive labeling in the central nucleus and hypothalamus. It is unlikely that this labeling was a consequence of infection of the superior salivatory nucleus as these structures all contained infected neurons at early time points and in the absence of infection in the salivatory nucleus.

Infection of the nucleus ambiguus

In general, the pattern of first-order infection of neurons in the medulla supports the contention that the laryngeal injection protocol employed directs virus to motor nerve endings in the TA muscle. The infection of neurons in the ipsilateral NA initially involved the loose formation as predicted by previous single retrograde labeling experiments from the TA (Hinrichsen and Ryan, 1981; Hinrichsen and Ryan, 1982; Portillo and Pasaro, 1988). At the earliest sampled times, and in most cases, infected cells were only located in the caudal loose formation, from approximately the level of the obex to about 700μM caudal to obex, and were usually arranged in scattered clumps. Unilateral section of the recurrent laryngeal nerve (or the vagus below the level of the superior laryngeal nerve) abolished ipsilateral infection in the NAl consistent with the determination that motorneurons in this portion of the NA send their axons through the RLN (Bieger and Hopkins, 1987; Hinrichsen and Ryan, 1981).

Two observations concerning viral infection of the NA from TA inoculation, however, are not consistent with previous retrograde tracing studies. First, by late day 4, infected neurons were present in the compact portion (and occasionally the semi-compact) of the NA even though motor neurons in these areas do not innervate the laryngeal musculature (Bieger and Hopkins, 1987. Previous studies (Bieger and Hopkins, 1987) have indicated that the NAc contains motor neurons innervating the cervical esophagus and the axons of NAc neurons run in the superior laryngeal nerve. Significantly, section of the SLN did not abolish infection of NAc after TA inoculation. This effectively rules out contamination of either the esophagus or cricothyroid as the likely source of NAc infection and suggests that the presence of infected cells is the result of direct or indirect transneuronal viral transport from the NAl. Motorneurons in the rostral NA (NAc and NAsc) are labeled by retrograde tracer injections made into the caudal NA (Nunez-Abades et al., 1990; ter Horst et al., 1984) though details of these connections are sketchy and they could represent connections to and/or within the adjacent reticular formation. The rostral dorsal portion of the NA, i.e. the NAc in rodents, and adjacent reticular areas are thought to contain one of the central pattern generators involved in swallowing, particularly the esophageal phase (Amirali et al., 2001; Jean, 1984; Jean, 2001). Glottic closure occurs during both pharyngeal and esophageal phases of swallowing (Shaker, 1995). It is possible that the (restricted) infection of the NAc and NAsc subsequent to NAl infection reflects virus moving along intrinsic connections that directly coordinate activity in the pharynx, esophagus and thyroarytenoid muscle (Altschuler, 2001).

In contrast to previous retrograde tracing studies using horseradish peroxidase (Hinrichsen and Ryan, 1981) or fluorescent dyes (Portillo and Pasaro, 1988), who reported exclusively ipsilateral NA labeling from laryngeal muscles, we consistently observed infection of neurons in the NAl contralateral to the inoculated TA muscle. Contralateral NA infection appeared at least 24 hours later than ipsilateral infection, and persisted after unilateral vagal, RLN and SLN section. In the cases with bilateral infection, transneuronal labeling was always heaviest ipsilaterally, and more structures were infected on the injected side. While this is suggestive of a minor bilateral innervation for the TA the possibility exists that intralaryngeal viral spread

occurred that we could not detect. Also, several studies (ter Horst et al., 1984) have reported contralateral NA labeling following retrograde tracer injections into the NA. Spread of virus via intramedullary connections with the opposite NA or adjacent reticular formation could account for the contralateral NA infection.

Transneuronal infection of laryngeal premotor neurons in the pons and medulla

The overall pattern of spread of infection subsequent to infection of NA neurons was remarkably consistent across animals with the same survival time and was little different between sympathectomized and intact animals. Variation was present largely in the numbers of infected cells in a given structure rather than the presence or absence of infection in that structure. Progression of infection to premotor (second-order infected) neurons could be parsed out through the differences in infected structures between 3 day animals (which had only motor neuron labeling) and 4 day animals which showed expansion of infected structures. Some refinement of the likely progression of infection was possible because early 4 day cases had fewer infected structures than late 4 day cases.

A significant number of the pontomedullary structures reported here as infected after TA inoculation in sympathectomized animals, e.g. the nucleus gigantocellularis and A7 group, have been reported to be infected after PRV inoculation of the kidney (Cano et al., 2004), brown adipose tissue (Cano et al., 2003), colon (Valentino et al., 2000), adrenal gland (Strack et al., 1989b) and presumably this reflects involvement of circuits concerned in sympatho-motor control. Other infected pontomedullary structures, notably the parvocellular reticular formation, have been reported to be infected following PRV inoculation of oro-facial muscles (Fay and Norgren, 1997a,b,c), presumably reflecting the presence of central pattern generators with outputs directed at multiple craniofacial motor nuclei. However, TA inoculation of PRV resulted in infection in two areas not reported in either of these two groups of studies; the NTS and the ventral respiratory column.

The earliest structure seen to be infected after the NA was the NTS; infected neurons were seen in the interstitial and central subnuclei in several animals with survival times under 72 hours. Increased numbers of infected cells in the cNTS, as well as in the interstitial, medial and intermediate NTS were seen in animals surviving 72–96 hours suggesting second-order spread from the NA. The central subnucleus of the NTS is the source of a strong projection to the NA (Cunningham and Sawchenko, 1989) which terminates in the compact portion only. In all 4 day cases, the NAc contained infected neurons suggesting strongly that the cNTS labeling resulted from NAc infection. However, a small number of infected cells were found in the NTS in two cases with <72 hours survival – and no NAc infection-, and in cases with SLN section, there was a significant reduction in the numbers of infected cNTS neurons ipsilateral to the nerve cut though infected cells were present in the ipsilateral NAc (Table 2). This raises the possibility that some portion of the infected cells in the cNTS became so through trans-*ganglionic* spread of PRV along afferent fibers running in the SLN. Indeed, the cNTS is the site of termination of some laryngeal afferents in addition to the dominant esophageal afferent input (Altschuler et al., 1989; Bellingham and Lipski, 1992). However, we were unable to consistently find infected cells in the nodose ganglion at 2 and 3 days post-inoculation (Fig. 1C).

In the 4 day (72–96 hour) cases, infected cells were additionally observed in the intermediate and interstitial NTS subdivisions bilaterally. These subdivisions receive substantial input from the SLN (Altschuler et al., 1989) and are known from viral tracing experiments to be premotor to esophageal and pharyngeal neurons (Bao et al., 1995; Barrett et al., 1994). The central, interstitial and intermediate subnuclei are activated in rodents during swallowing induced by SLN stimulation (Sang and Goyal, 2001). In the cat ((Ambalavanar et al., 2004), the interstitial subnucleus is the principle NTS region activated (bilaterally) during SLN stimulation-induced

movements of the TA without swallowing. It is possible that the interstitial subnucleus was infected directly from the TA motorneurons in the NAl but in all cases reported here, infected neurons in these subdivisions were accompanied by infected cells in the NAc, which cannot be discounted as a source of interstitial NTS infection.

Overall, these findings are consistent with previous anatomical and viral studies showing that the NTS contains cells in its intermediate, interstitial and central subnuclei that are directly premotor to NA motorneurons. However, the data are inconclusive about direct NTS innervation of the restricted subset of TA motorneurons in the NAl. It is possible that TA motorneurons in the NAl are not innervated directly by the NTS at all- they certainly appear not to be by the cNTS (Cunningham and Sawchenko, 1989) – but are tied into the disynaptic reflex circuits involving the NTS that heavily influence esophageal and pharyngeal motorneurons in the TA (Ambalavanar et al., 2004).

The ventral respiratory column of the reticular formation neurons extends from the caudal border of the facial nucleus to the spinomedullary junction in rats and consists of three main divisions (Alheid et al., 2002). The rostrally-situated Bötzinger complex and the caudal ventral respiratory group (nucleus retroambigualis) both contain many neurons premotor to phrenic motorneurons (Dobbins and Feldman, 1994) and both areas contain mostly expiration related neurons (Ezure et al., 1988). Neurons in both areas send axons to the nucleus ambiguus with a heavier innervation of the NA caudal to the obex (Saito et al., 2002). The caudal ventral respiratory group incorporates the nucleus retroambigualis (Ezure et al., 1988; Saito et al., 2002), a key structure for coordinating laryngeal, thoracic and abdominal muscles in complex behaviors like vocalization, defecation and coughing (Boers et al., 2002; Holstege, 1989).

Small numbers of infected neurons were first observed in the Bötzinger complex and caudal VRG/NRA at 72–84 hours after PRV injections into the TA (Fig. 2A). This is consistent with direct innervation of NA motorneurons by the Bötzinger complex and caudal VRG reported in the rat (Saito et al., 2002), and with a similar direct innervation by the nucleus retroambigualis reported in primates (VanderHorst et al., 2001). At later times (96–120 hours post-inoculation) a large proportion of the cells in the Bötzinger complex were infected (Fig. 2C) possibly through projections to the NAc or through intrinsic connections. The pre-Bötzinger complex (Alheid et al., 2002), which contains mostly inspiratory-related neurons, was conspicuous by its lack of infected cells even at post-infection times in excess of 120 hours (Fig. 7B). In humans the TA muscle is mostly active during expiration (Kuna et al., 1988).

At around 84–96 hours post-inoculation, small numbers of infected cells were identifiable in the pontomedullary reticular formation ipsilateral to the inoculation site. The majority of these cells was located in the dorsal parvicellular region that extends from the caudal end of the motor trigeminal nucleus to the hypoglossal nucleus. After 96 hours, increased numbers of infected cells were present in the ipsilateral PCRT and in smaller numbers in the contralateral PCRT. By 120 hours post-inoculation, infection of the PCRT was bilateral and symmetrical in terms of infected cell number (Fig. 7C). The origin of the infection in the PCRT is difficult to identify precisely (and may be from multiple sources) but several lines of evidence suggest that it is from second-order infected cells in the respiratory and swallowing centers, and from the contralateral PCRT itself. First, PCRT infection was never seen in cases with survival times less than 84 hours despite infection of the NA (in some cases both NAc and NAl), NTS and ventrolateral reticular formation. At a minimum, this suggests that the PCRT is not among the medullary populations directly connected to the NA. Second, in cases with section of the vagus or RLN ipsilateral to the viral inoculation site, ipsilateral PCRT infection occurred without ipsilateral NA infection though the contralateral PCRT was infected. Third, PCRT infection occurs after PRV injections into the jaw, tongue and facial muscles (Fay and Norgren, 1997a;Fay and Norgren, 1997b;Fay and Norgren, 1997c) as well as the viscera via their

sympathetic innervation (Strack et al., 1989a). Taken together, these findings suggest that neurons in the PCRT innervate neurons premotor to cranial nerve motor nuclei and pre-ganglionic sympathetic neurons.

Third-order neurons related to TA motorneurons

Around 96 hours post-inoculation it was evident that infection in the medulla was spreading outside of areas shown by single-connection tracing techniques to be directly premotor to NA motorneurons (Table 1). The main form of this spread was the appearance of infected neurons in the midbrain, hypothalamus, amygdala and cortex. Definitive designation of newly infected areas as third-order areas, i.e. infected from second-order neurons, is complicated by the fact that retrograde transport of virus and replication may proceed at different rates in different neurons (Smith et al., 2000) and many descending systems are connected in a parallel manner or have extensive collaterals. Infection of higher-order structures may thus have multiple origins. Nonetheless, it was possible to identify consistently labeled areas and trace the likely origin of infection. Four main areas were identified:

Midbrain

Infected cells were identifiable in the substantia nigra (both partes reticulata and compacta), pedunculopontine tegmentum and the periaqueductal gray by 96 hours post-inoculation of PRV into the TA muscle. The SNr innervates PCRT premotor neurons directly (Yasui et al., 1995; Yasui et al., 1997). In the PAG, infected cells were initially largely restricted to the lateral part of the ventrolateral column at caudal levels. This is consistent with several retrograde and anterograde tracing studies in cat and monkey (Holstege, 1989; Jurgens, 2002) showing innervation of the nucleus retroambigualis/caudal respiratory by cells in the ventrolateral PAG. These studies failed to find direct innervation of the NA itself, and the present data show that in the rat this is also likely the case as PAG infection did not occur until infection had spread from the NA to the adjacent reticular formation. At 5 day sample points, infected neurons were also observed in the dorsolateral cell column and were present in the rostral PAG (Figs. 3C and D). It is not clear how these cells became infected but it is worth noting that in the guinea pig, different types of vocalization can be elicited from rostral/dorsolateral and caudal/ventrolateral PAG (Kyuhou and Gemba, 1998).

Hypothalamus

Infection of the hypothalamus appeared to occur in two phases. Initially, infected neurons could be identified in the lateral hypothalamus, the parvocellular and posterior portions of the paraventricular nucleus, and the preoptic area at between 84 and 96 hours post-inoculation (Fig. 6) The first two areas have strong connections with medullary autonomic, gustatory and viscerosensory areas, most notably the NTS and dorsal vagal motor nucleus (e.g. ter Horst et al., 1984). Since the NTS was always infected prior to infection in the hypothalamus, it must be considered a likely source of transneuronal infection in the paraventricular and lateral areas. However, both the lateral hypothalamus and the parvocellular division of the paraventricular nucleus can be infected by pseudorabies virus injected into (sympathectomized) hind limb muscles without involvement of the NTS (Kerman et al., 2006). It has been proposed that subsets of neurons in the LH and PVN (as well as the dorsomedial and dorsolateral hypothalamus) are involved in coordinating sympathetic and motor activity during emotionally driven behaviors through collateralized innervation of spinal pre-ganglionic and motor neurons (Kerman et al., 2003;Kerman et al., 2006). Though there is no evidence that the LH or PVN directly innervate bulbar motor neurons, the presence of PRV in these areas after TA inoculation suggests a hypothalamic sympatho-motor coordinating system exists for laryngeal muscles. This is also supported by the fact that sympathectomy failed to abolish infection of the LH and PVN after TA inoculation though there was a major attenuation of infection in the

perifornical region (Fig. 7A and B). Tracing studies (e.g. ter Horst et al., 1984; Ciriello et al., 2003) have reported retrograde labeling in the lateral hypothalamus and perifornical area following injection of HRP or fluorescent tracers into the NA.

Infected cells were consistently seen in the medial and lateral preoptic areas after TA injection of PRV in both sympathectomized and non-sympathectomized animals beginning at day 4. Neurons in the ventrolateral preoptic area, which were consistently seen infected by 96 hours post-inoculation, are involved in the homeostatic regulation of sleep (Sherin et al., 1996). Maintenance of glottic opening is essential during sleep and the TA is phasically active during REM sleep (Kuna et al., 1988). However, there is no evidence that neurons in the VLPO project directly to the NA or adjacent related reticular formation (ter Horst et al., 1984; Steininger et al., 2001) though a projection from the VLPO to the medulla just ventrolateral to the NA has been described (Sherin et al., 1998). Interestingly, numerous infected neurons in the ventral tuberomammillary nucleus, and median preoptic area were identified in late day 4 cases suggesting, in the absence of direct projections from this nucleus to the NA (e.g. Ciriello et al., 2003), that infection spread retrogradely from the VLPO to these afferent sources (Chou et al., 2002).

Amygdala

Infection in the amygdala has been reported following PRV injections into the posterior cricoarytenoid muscle (Waldbaum et al., 2001) but not other skeletal muscles. Infection of the ipsilateral central nucleus was evident by 96 hours post-inoculation, and at later time points, infection had spread within the central nucleus itself. The central nucleus is part of a larger brain structure, the extended amygdala, that includes the sublenticular substantia innominata and bed nucleus of the stria terminalis (Alheid et al., 2002). Both these latter structures contained infected cells by 120 hours post-inoculation but were never seen in advance of infection of the central nucleus itself.

The central nucleus is the only amygdaloid nucleus with projections to the midbrain, pons and medulla. Central nucleus axons innervate the A1 noradrenergic cell group, the rostral, central, commissural and ventral NTS in the dorsal medulla, the A6 (subceruleus) and parabrachial complex in the pons, and the substantia nigra, pars compacta, dorsal raphe and periaqueductal gray in the midbrain (Wallace et al., 1992; Danielson et al., 1989). Infection of Ce neurons could have arisen from infection of these cell groups as well as the lateral hypothalamus. However, a large number of axons and axon terminals from the Ce end in the parvicellular reticular formation (Yasui et al., 2004) and given the early onset of Ce infection, this medullary region must be considered a likely source.

The Ce is widely considered to be responsible for generating or modulating autonomic and somatic responses to stimuli conditioned to aversive stimuli, i.e. conditioned responses (Cardinal et al., 2002). Though there are no data linking the Ce directly to alterations in laryngeal function *per se*, the Ce is required for the acquisition and expression of conditioned vocalizations (Borszcz and Leaton, 2003).

Cortex

Neurons with detectable PRV infection first appeared in cortex at about 96 hours after inoculation and were restricted to layer V of the ipsilateral granular and dysgranular parietal insular cortex roughly at or caudal to the level of bregma. The gustatory representation in the posterior insula extends from approximately bregma to 1.5mm rostral to bregma and there is a distinct transition to visceral-related cortex around the level of bregma (Krushel and van der Kooy, 1988; Allen et al., 1991). Initial restriction of infection of gPA/dPA after TA inoculation to neurons in their most rostral portions may relate to the presence of a distinct larynx

representation in this viscerosensory cortical area. The relatively early origin of the initial insular infection suggests that it originated in the PCRT or the NTS, both of which receive direct input from layer V of the insular cortex (Van der Kooy et al., 1984; Zhang and Sasamoto, 1990; Allen et al., 1991). As indicated in Fig. 9B, a second area of infected layer V neurons appeared in the parietal insular cortex (at around 2mm behind bregma) at 5 days p.i. The parietal insular cortex is that part of the insular cortex that receives somatosensory input from the second somatosensory area and the posterior thalamus (Shi and Cassell, 1998b). The origin of this second layer V infection in the PA is unclear though a subcortical origin is likely: possibilities include the spinal nucleus of the trigeminal nerve and the cuneate nucleus which consistently contained infected neurons by this time point. However, the most likely possibility is retrograde infection from subcortical autonomic-related sites, notably the NTS. The rat insular cortex from roughly 1.25 and 1.5mm behind bregma receives baroreceptor- related input (Zhang and Oppenheimer, 2000a; Zhang and Oppenheimer, 2000b) that is originally transferred from the vagus nerve to the CNS via the medial and commissural divisions of the NTS. Both these areas contained PRV-GFP immunopositive neurons by early day 5, presumably as a result of virus movement through intrinsic NTS connections.

By 120 hours post-inoculation, infection was present bilaterally in the dysgranular insular cortices, and in the ipsilateral dPI, infected cells were now present in layers II and III. In addition, all 5 day cases now had infected cells in the agranular posterior (aPI), dysgranular anterior (dAI) and parietal insular cortices). Both the aPI and dAI are reciprocally connected with the dPA (Shi and Cassell, 1998a,b) and are likely to have become infected by virus spreading retrogradely through corticocortical connections. Dysgranular AI is also connected with head and forelimb regions of motor cortex and has been proposed to be an interface between the insula and the motor system (Shi and Cassell, 1998a). In monkeys, the motor cortical larynx area in the inferior precentral cortex is heavily reciprocally connected with the insula while also projecting to motor cortex (Simonyan and Jurgens, 2002 Simonyan and Jurgens, 2005). These connectional similarities, plus its extreme lateral location, suggest that dAI may be homologous the motor cortical larynx area in the monkey.

PRV infected cells were observed bilaterally in the medial prefrontal cortex just dorsal to the genu of the corpus callosum. The area of infection, which was fairly circumscribed, appeared to be located in the dorsal prelimbic region of Gabbott (Gabbott et al.,2005) though elsewhere this region has been designated cingulate area (CG) 2 (Paxinos and Watson) or ventral anterior cingulate. Whatever the designation, the infected cells appeared to be in regions that project to the periaqueductal gray and caudal ventrolateral medulla (Gabbott et al., 2005). The ventral cingulate/dorsal prefrontal region is the cortical origin of the vocalization pathway in primates and other species (Holstege, 1989; Jurgens, 2002). In rodents, stimulation of the dorsal prelimbic area consistently elicits 50kHz ultrasonic vocalizations (Burgdorf et al., 2007). The ventral anterior cingulate cortex innervates cells in the VRG/NRA (Jurgens and Hage, 2005) that are premotor to the NA: infection was present in the VRG/NRA here in cases with CG2 infection (Fig. 6C) though the ventrolateral PAG was also heavily infected.

Contralateral motor cortex (M1) only contained infected cells in animals with post-inoculation survival times in excess of 120 hours. The number of cells was generally small (2–8 per section) and restricted to layer V. Corticobulbar neurons from motor areas in the rat have been reported to indirectly innervate motor neurons so the late appearance of infection in M1 could be related to a slower transport rate of virus across multiple synapses in this connection. However, infection of layer V neurons in a restricted part M1/M2 has been reported following PRV inoculation of the heart (ter Horst et al., 1996) and brown adipose tissue (Cano et al., 2003). A possible explanation for this is infection of the rubrospinal pathway and/or pre-rubral fields (Cano et al., 2003). A number of PRV infected cells in the retrorubral area were consistently seen following TA inoculation and this could account for the motor cortex labeling.

Conclusions: Central forebrain systems controlling the thyroarytenoid muscle

Despite a number of ambiguities in the source of infection in some areas, the data indicate a trend for PRV to spread along three distinct interconnected supra-bulbar systems following infection of the nucleus ambiguus by PRV inoculation of the thyroarytenoid. The anterior cingulate cortex, periaqueductal gray and ventral respiratory group which form the main components of the vocalization pathway in mammals (Jurgens, 2002) were all infected following TA PRV inoculation. In addition, the present data indicate that TA is strongly connected to a second descending system interconnecting the viscerally-related parietal insular cortex, the amygdala, the lateral hypothalamus, and the parvocellular reticular formation. Rather than being related to autonomic function (Van der Kooy et al., 1984), this system may be better described as a branchiomotor system involved in coordinating complex movements like swallowing which almost exclusively involve muscles of branchial arch origin. This coordination is probably achieved by influencing pattern generators embedded in the PCRT (Jean, 2001). Finally, the data support a strong interconnection between the TA muscle and selective groups of hypothalamic nuclei, in particular those involved in sympatho-motor coordination and sleep.

Acknowledgments

SUPPORTED BY GRANT: NIH 5K08DC6931

Abbreviations used

aAI
agranular anterior insular cortex

ac
anterior commissure

AHA
anterior hypothalamic area

AP
area postrema

aq
cerebral aqueduct

aPA
agranular parietal insular cortex

aPI
agranular posterior insular cortex

ARYC
arytenoids cartilage

BNST
bed nucleus of the stria terminalis

BotzC/BzC
Bötzinger complex

CG1–3
cingulate areas 1–3

CeL lateral division of central nucleus of amygdala

CeM medial division of central nucleus of amygdala

cereb cerebellum

CGRP calcitonin gene-related peptide

ChAT choline acetlytransferase

cNTS central division of NTS

comNTS commissural NTS

cp caudate-putamen

DAB 3, 3′diaminobenzidine

dAI dysgranular anterior insular cortex

d dorsal subnucleus of PAG

DCN dorsal cochlear nucleus

dl dorsolateral subnucleus of PAG

dlNTS dorsolateral division of NTS

DM dorsomedial hypothalamic nucleus

DMD dorsal division, dorsomedial hypothalamic nucleus

dPA dysgranular parietal insular cortex

dPI dysgranular posterior insular cortex

DR dorsal raphe

DTg dorsal tegmental nucleus

DK
nucleus of Darkschewitsch

DPGi
dorsal nucleus paragigantocellularis

ENT
entorhinal cortex

fx
fornix

GFP
green fluorescent protein

Gi
nucleus gigantocellularis

gPA
granular parietal insular cortex

gPI
granular posterior insular cortex

gVII
genu of facial nerve

HDB
horizontal limb, diagonal band of Broca

ICON
inferior constrictor

ICP
inferior cerebellar peduncle

inNTS
intermediate division of NTS

IO
inferior olive

IRT
intermediate reticular formation

isNTS
interstitial NTS

LC
locus ceruleus

LCA
lateral cricoarytenoid muscle

LDTg
lateral dorsal tegmental nucleus

LH
lateral hypothalamus

LM lateral mammillary nucleus

LPB lateral parabrachial nuclei

LPO lateral preoptic area

LRT lateral reticular nucleus

LSO lateral superior olive

Lve lateral vestibular nucleus

m medial subnucleus of PAG

M1 first motor cortex

MCA middle cerebral artery

MDv medullary reticular field, ventral part

meV mesencephalic nucleus of trigeminal nerve

moV motor nucleus of trigeminal nerve

MMN medial mammillary nuclei

MPA medial preoptic area

MPB medial parabrachial nuclei

MPO medial preoptic nucleus

mNTS medial division of NTS

MnPO median preoptic nucleus

mt mammillothalamic tract

Mve medial vestibular nucleus

NA
nucleus ambiguous

Nac
nucleus ambiguus, compact part

Nal
nucleus ambiguus, loose part

Nasc
nucleus ambiguus, semicompact part

Ncu
cuneate nucleus

NGr
gracile nucleus

NIII
oculomotor nucleus

Nphr
phrenic nucleus

NRA
nucleus retroambigualis

NTS
nucleus tractus solitarii

NVII
facial nucleus

nVII
facial nerve

NX
dorsal motor nucleus of vagus

NXII
hypoglossal nucleus

ot
optic tract

ox
optic chiasm

PAG
periaqueductal gray

PCA
posterior cricoarytenoid muscle

PCRT
parvocellular reticular formation

PCRTa
alpha subregion of the PCRT

Pe
periventricular region of hypothalamus

PeF
perifornical region of hypothalamus

PerO
periolovary region

PH
posterior hypothalamic nucleus

PIR
piriform cortex

plac
posterior limb, anterior commissure

PM
posteromedial hypothalamus

PnC
nucleus pontis caudalis

PnN
pontine nuclei

PnO
nucleus pontis oralis’

PPTg
peduculopontine tegmentum

PR
perirhinal cortex

PVNp
posterior division, paraventricular hypothalamic nucleus

PVNpo
parvocellular division, paraventricular hypothalamic nucleus

Prb
Probst’s nucleus

preBOTZC
preBötzinger comples

PrH
nucleus prepositus hypoglossi

PRV
pseudorabies virus

PrV
principal nucleus of trigeminal nerve

PVAB
parvalbumin

Robs nucleus raphe obscurus

RPn nucleus raphe pontis

rs rhinal sulcus

RVL rostral ventrolateral medulla

S2 second somatosensory area

SI substantia innominata

SNc substantia nigra, pars compacta

SNr substantia nigra, pars reticulata

SnV sensory root of trigeminal nerve

SON supraoptic nucleus

spV spinal tract of trigeminal nerve

SpV spinal nucleus of trigeminal nerve

SpVc pars caudalis of SpV

SpVe spinal vestibular nucleus

SpVi pars intermedialis of SpV

SpVo pars oralis of SpV

ST subthalamic nucleus

st stria terminalis

SubC subceruleus region

SuM supramammillary nuclear complex

SuVe
superior vestibular nucleus

TA
thyroarytenoid muscle

Te3
third temporal cortical area

THYRC
thyroid cartilage

ts
tractus solitarius

TuM
tuberomammillary nucleus

VCN
ventral cochlear nucleus

vl
ventrolateral subnucleus of PAG

vlNTS
ventrolateral division of NTS

VLPO
ventrolateral preoptic area

VMH
ventromedial hypothalamic nucleus

VRG
entral respiratory group

Xscp
decussation of superior cerebellar peduncle

References

Alheid GF, Gray PA, Jiang MC, Feldman JL, McCrimmon DR. Parvalbumin in respiratory neurons of the ventrolateral medulla of the adult rat. J Neurocytol 2002;31:693–717. [PubMed: 14501208]

Allen GV, Saper CB, Hurley KM, Cechetto DF. Organization of visceral and limbic connections in the insular cortex of the rat. J Comp Neurol 1991;311:1–16. [PubMed: 1719041]

Altschuler SM, Bao XM, Bieger D, Hopkins DA, Miselis RR. Viscerotopic representation of the upper alimentary tract in the rat: sensory ganglia and nuclei of the solitary and spinal trigeminal tracts. J Comp Neurol 1989;283:248–268. [PubMed: 2738198]

Altschuler SM, Bao XM, Miselis RR. Dendritic architecture of nucleus ambiguus motoneurons projecting to the upper alimentary tract in the rat. J Comp Neurol 1991;309:402–414. [PubMed: 1717520]

Altschuler SM. Laryngeal and respiratory protective reflexes. Am J Med 2001;111(Suppl 8A):90S–94S. [PubMed: 11749932]

Ambalavanar R, Tanaka Y, Selbie WS, Ludlow CL. Neuronal activation in the medulla oblongata during selective elicitation of the laryngeal adductor response. J Neurophysiol 2004;92:2920–2932. [PubMed: 15212423]

Amirali A, Tsai G, Schrader N, Weisz D, Sanders I. Mapping of brain stem neuronal circuitry active during swallowing. Ann Otol Rhinol Laryngol 2001;110:502–513. [PubMed: 11407840]

Bao X, Wiedner EB, Altschuler SM. Transsynaptic localization of pharyngeal premotor neurons in rat. Brain Res 1995;696:246–9. [PubMed: 8574676]

Barrett RT, Bao X, Miselis RR, Altschuler SM. Brain stem localization of rodent esophageal premotor neurons revealed by transneuronal passage of pseudorabies virus. Gastroenterology 1994;107:728–37. [PubMed: 8076758]

Bauman NM, Wang D, Jaffe DM, Porter MP, McCulloch TM, Smith RJ, Sandler AD. Role of substance P in the laryngeal chemoreflex. Ann Otol Rhinol Laryngol 1998 Jul;107(7):575–80. [PubMed: 9682852]

Bellingham MC, Lipski J. Morphology and electrophysiology of superior laryngeal nerve afferents and postsynaptic neurons in the medulla oblongata of the cat. Neuroscience 1992;48:205–216. [PubMed: 1374862]

Bieger D, Hopkins DA. Viscerotopic representation of the upper alimentary tract in the medulla oblongata in the rat: the nucleus ambiguus. J Comp Neurol 1987;262:546–562. [PubMed: 3667964]

Boers J, Klop EM, Hulshoff AC, de Weerd H, Holstege G. Direct projections from the nucleus retroambiguus to cricothyroid motoneurons in the cat. Neurosci Lett 2002;319:5–8. [PubMed: 11814640]

Borszcz GS, Leaton RN. The effect of amygdala lesions on conditional and unconditional vocalizations in rats. Neurobiol Learn Mem 2003;79:212–25. [PubMed: 12676520]

Card JP, Enquist LW. Transneuronal circuit analysis with pseudorabies viruses. Curr Protoc Neurosci 2001;Chapter 1(Unit15)

Card JP, Rinaman L, Lynn RB, Lee BH, Meade RP, Miselis RR, Enquist LW. Pseudorabies virus infection of the rat central nervous system: ultrastructural characterization of viral replication, transport, and pathogenesis. J Neurosci 1993;13:2515–2539. [PubMed: 8388923]

Cardinal RN, Parkinson JA, Hall J, Everitt BJ. Emotion and motivation: the role of the amygdala, ventral striatum, and prefrontal cortex. Neurosci Biobehav Rev 2002;26:321–352. [PubMed: 12034134]

Cunningham ET Jr, Sawchenko PE. A circumscribed projection from the nucleus of the solitary tract to the nucleus ambiguus in the rat: anatomical evidence for somatostatin-28-immunoreactive interneurons subserving reflex control of esophageal motility. J Neurosci 1989;9:1668–1682. [PubMed: 2470875]

Dobbins EG, Feldman JL. Brainstem network controlling descending drive to phrenic motoneurons in rat. J Comp Neurol 1994;347:64–86. [PubMed: 7798382]

Ertekin C, Palmer JB. Physiology and electromyography of swallowing and its disorders. Suppl Clin Neurophysiol 2000;53:148–154. [PubMed: 12740989]

Ezure K, Manabe M, Yamada H. Distribution of medullary respiratory neurons in the rat. Brain Res 1988;455:262–270. [PubMed: 3401782]

Fay RA, Norgren R. Identification of rat brainstem multisynaptic connections to the oral motor nuclei in the rat using pseudorabies virus. II. Facial muscle motor systems. Brain Res Brain Res Rev 1997a; 25:276–290. [PubMed: 9495559]

Fay RA, Norgren R. Identification of rat brainstem multisynaptic connections to the oral motor nuclei using pseudorabies virus. I. Masticatory muscle motor systems. Brain Res Brain Res Rev 1997b; 25:255–275. [PubMed: 9495558]

Fay RA, Norgren R. Identification of rat brainstem multisynaptic connections to the oral motor nuclei using pseudorabies virus. III. Lingual muscle motor systems. Brain Res Brain Res Rev 1997c;25:291–311. [PubMed: 9495560]

Hinrichsen CF, Ryan A. The size of motor units in laryngeal muscles of the rat. Experientia 1982;38:360–361. [PubMed: 6176466]

Hinrichsen CF, Ryan AT. Localization of laryngeal motoneurons in the rat: morphologic evidence for dual innervation? Exp Neurol 1981;74:341–355. [PubMed: 6170521]

Holstege G. Anatomical study of the final common pathway for vocalization in the cat. Journal of Comparative Neurology 1989;284:242–52. [PubMed: 2754035]

Inagi K, Schultz E, Ford CN. An anatomic study of the rat larynx: establishing the rat model for neuromuscular function. Otolaryngol Head Neck Surg 1998;118:74–81. [PubMed: 9450832]

Jansen AS, Farwell DG, Loewy AD. Specificity of pseudorabies virus as a retrograde marker of sympathetic preganglionic neurons: implications for transneuronal labeling studies. Brain Res 1993;617:103–112. [PubMed: 8397044]

Jean A. Brain stem control of swallowing: neuronal network and cellular mechanisms. Physiological Reviews 2001;81:929–69. [PubMed: 11274347]

Jean A. Brainstem organization of the swallowing network. Brain Behav Evol 1984;25:109–116. [PubMed: 6100081]

Jurgens U. Neural pathways underlying vocal control. Neuroscience & Biobehavioral Reviews 2002;26:235–58. [PubMed: 11856561]

Kerman IA, Enquist LW, Watson SJ, Yates BJ. Brainstem substrates of sympatho-motor circuitry identified using trans-synaptic tracing with pseudorabies virus recombinants. J Neurosci 2003;23:4657–4666. [PubMed: 12805305]

Kerman IA, Shabrang C, Taylor L, Akil H, Watson SJ. Relationship of presympathetic-premotor neurons to the serotonergic transmitter system in the rat brainstem. J Comp Neurol 2006;499:882–896. [PubMed: 17072838]

Krushel LA, van der Kooy D. Visceral cortex: integration of the mucosal senses with limbic information in the rat agranular insular cortex. J Comp Neurol 1988;270:39–54. 62–3. [PubMed: 2453537]

Lobera B, Pasaro R, Gonzalez-Baron S, Delgado-Garcia JM. A morphological study of ambiguus nucleus motoneurons innervating the laryngeal muscles in the rat and cat. Neurosci Lett 1981;23:125–130. [PubMed: 7254697]

Ludlow CL. Central nervous system control of the laryngeal muscles in humans. Respir Physiol Neurobiol 2005;147:205–222. [PubMed: 15927543]

McCulloch TM, Perlman AL, Palmer PM, Van Daele DJ. Laryngeal activity during swallow, phonation, and the Valsalva maneuver: an electromyographic analysis.[erratum appears in Laryngscope 1997 Jan;107(1):146]. Laryngoscope 1996;106:1351–8. [PubMed: 8914900]

Nunez-Abades PA, Portillo F, Pasaro R. Characterisation of afferent projections to the nucleus ambiguus of the rat by means of fluorescent double labelling. J Anat 1990;172:1–15. [PubMed: 2272895]

Paxinos, G.; Watson, C. The rat brain in stereotaxic coordinates. Sydney ; Orlando; New York: Academic Press; 2005. p. 456

Perlman AL, Palmer PM, McCulloch TM, Vandaele DJ. Electromyographic activity from human laryngeal, pharyngeal, and submental muscles during swallowing. Journal of Applied Physiology 1999;86:1663–9. [PubMed: 10233133]

Poletto CJ, Verdun LP, Strominger R, Ludlow CL. Correspondence between laryngeal vocal fold movement and muscle activity during speech and nonspeech gestures. J Appl Physiol 2004;97:858–866. [PubMed: 15133000]

Portillo F, Pasaro R. Location of bulbospinal neurons and of laryngeal motoneurons within the nucleus ambiguus of the rat and cat by means of retrograde fluorescent labelling. J Anat 1988;159:11–18. [PubMed: 3248958]

Saito Y, Tanaka I, Ezure K. Morphology of the decrementing expiratory neurons in the brainstem of the rat. Neurosci Res 2002;44:141–153. [PubMed: 12354629]

Sang Q, Goyal RK. Swallowing reflex and brain stem neurons activated by superior laryngeal nerve stimulation in the mouse. Am J Physiol Gastrointest Liver Physiol 2001;280:G191–200. [PubMed: 11208540]

Sasaki CT, Suzuki M. Laryngeal reflexes in cat, dog, and man. Arch Otolaryngol 1976;102:400–402. [PubMed: 938318]

Shaker R. Airway protective mechanisms: current concepts. Dysphagia 1995;10:216–227. [PubMed: 7493501]

Shi CJ, Cassell MD. Cascade projections from somatosensory cortex to the rat basolateral amygdala via the parietal insular cortex. Journal of Comparative Neurology 1998a;399:469–91. [PubMed: 9741478]

Shi CJ, Cassell MD. Cortical, thalamic, and amygdaloid connections of the anterior and posterior insular cortices. Journal of Comparative Neurology 1998b;399:440–68. [PubMed: 9741477]

Smith BN, Banfield BW, Smeraski CA, Wilcox CL, Dudek FE, Enquist LW, Pickard GE. Pseudorabies virus expressing enhanced green fluorescent protein: A tool for in vitro electrophysiological analysis

of transsynaptically labeled neurons in identified central nervous system circuits. Proc Natl Acad Sci U S A 2000;97:9264–9269. [PubMed: 10922076]

Strack AM, Sawyer WB, Hughes JH, Platt KB, Loewy AD. A general pattern of CNS innervation of the sympathetic outflow demonstrated by transneuronal pseudorabies viral infections. Brain Res 1989a; 491:156–162. [PubMed: 2569907]

Strack AM, Sawyer WB, Platt KB, Loewy AD. CNS cell groups regulating the sympathetic outflow to adrenal gland as revealed by transneuronal cell body labeling with pseudorabies virus. Brain Res 1989b;491:274–296. [PubMed: 2548665]

Swanson, LW. Brain maps III : structure of the rat brain : an atlas with printed and electronic templates for data, models and schematics. Amsterdam ; Boston: Elsevier/Academic Press; 2004. p. 215

ter Horst GJ, Luiten PG, Kuipers F. Descending pathways from hypothalamus to dorsal motor vagus and ambiguus nuclei in the rat. J Auton Nerv Syst 1984;11:59–75. [PubMed: 6470410]

Terreberry RRNE. The rat medial frontal cortex projects directly to autonomic regions of the brainstem. Brain Res Bull 1987;19:639–649. [PubMed: 2449937]

Van Daele DJ, Cassell MD. Amygdala and insular connections to the larynx and tongue as determined by pseudorabies retrograde labeling. Society for Neuroscience. 2007

Van Daele DJ, Cassell MD. Cortical and subcortical laryngeal connections as determined by pseudorabies retrograde labeling. Society for Neuroscience. 2006

VanderHorst VG, Terasawa E, Ralston HJ 3rd. Monosynaptic projections from the nucleus retroambiguus region to laryngeal motoneurons in the rhesus monkey. Neuroscience 2001;107:117–125. [PubMed: 11744252]

Yasui Y, Tsumori T, Ando A, Domoto T. Demonstration of axon collateral projections from the substantia nigra pars reticulata to the superior colliculus and the parvicellular reticular formation in the rat. Brain Res 1995;674:122–126. [PubMed: 7539705]

Yasui Y, Tsumori T, Ono K, Kishi T. Nigral axon terminals are in contact with parvicellular reticular neurons which project to the motor trigeminal nucleus in the rat. Brain Res 1997;775:219–224. [PubMed: 9439848]

Zhang Z, Oppenheimer SM. Electrophysiological evidence for reciprocal insulo-insular connectivity of baroreceptor-related neurons. Brain Res 2000a;863:25–41. [PubMed: 10773190]

Zhang ZH, Oppenheimer SM. Baroreceptive and somatosensory convergent thalamic neurons project to the posterior insular cortex in the rat. Brain Res 2000b;861:241–256. [PubMed: 10760486]

Zhang J, Yang R, Pendlebery W, Luo P. Monosynaptic circuitry of trigeminal proprioceptive afferents coordinating jaw movement with visceral and laryngeal activities in rats. Neuroscience 2005;135:497–505. [PubMed: 16111816]

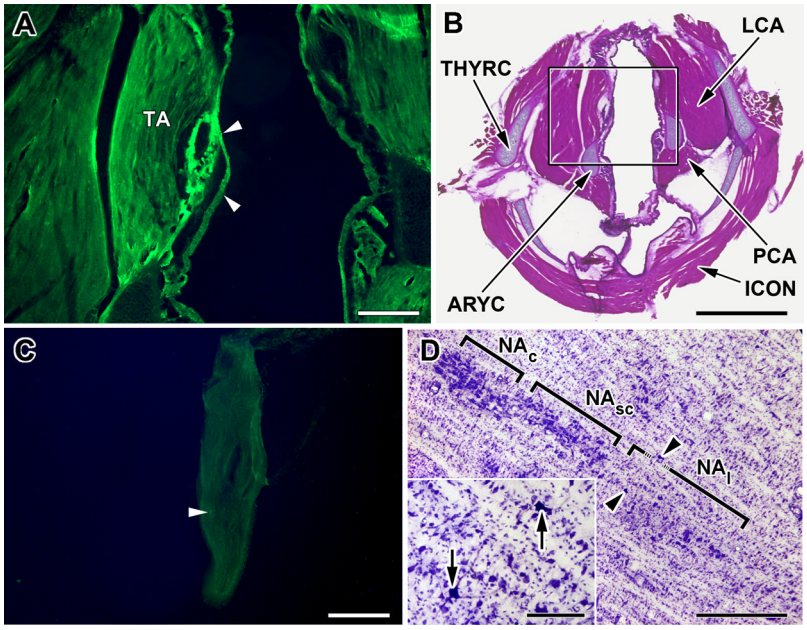

Figure 1.

Pseudorabies inoculation in the thyroarytenoid (TA) muscle and transport to the nucleus ambiguus.

A. Fluorescent micrograph of a tranverse section through the rat larynx showing typical site of inoculation (arrowheads) of PRV-GFP into the thyroarytenoid muscle (TA) 60 hours after inoculation. Scale bar: 200μM.

B. Low power photomicrograph of the section shown in A now counterstained with hemotoxylin and eosin. The attachment of the thyroarytenoid muscle (TA) to the thyroid (THYRC) and arytenoid (ARYC) cartilages can be seen, as can the relative locations of the posterior (PCA) and lateral (LCA) cricoarytenoid and the inferior constrictor (ICON) muscles. Black square outlines the image shown in A. Scale bar: 1mm

C. Fluorescent micrograph of a longitudinal section through the nodose ganglion from an animal inoculated with PRV-GFP 60 hours prior to sacrifice. Note that only a single GFP fluourescent neurons (arrowhead) in this section. Scale Bar: 200μM

D. Cresyl violet counterstained horizontal section, 50 μM thick, through the rat medulla showing initial infection of motor neurons (arrowheads; arrows in inset) in the loose portion of the nucleus ambiguus (NA_l) three days after inoculation of PRV into the TA. No infection was seen in the semi-compact (NA_{sc}) or compact (NA_c) parts of the nucleus ambiguus. Scale bar: 1mm; Scale bar in inset: 100μM.

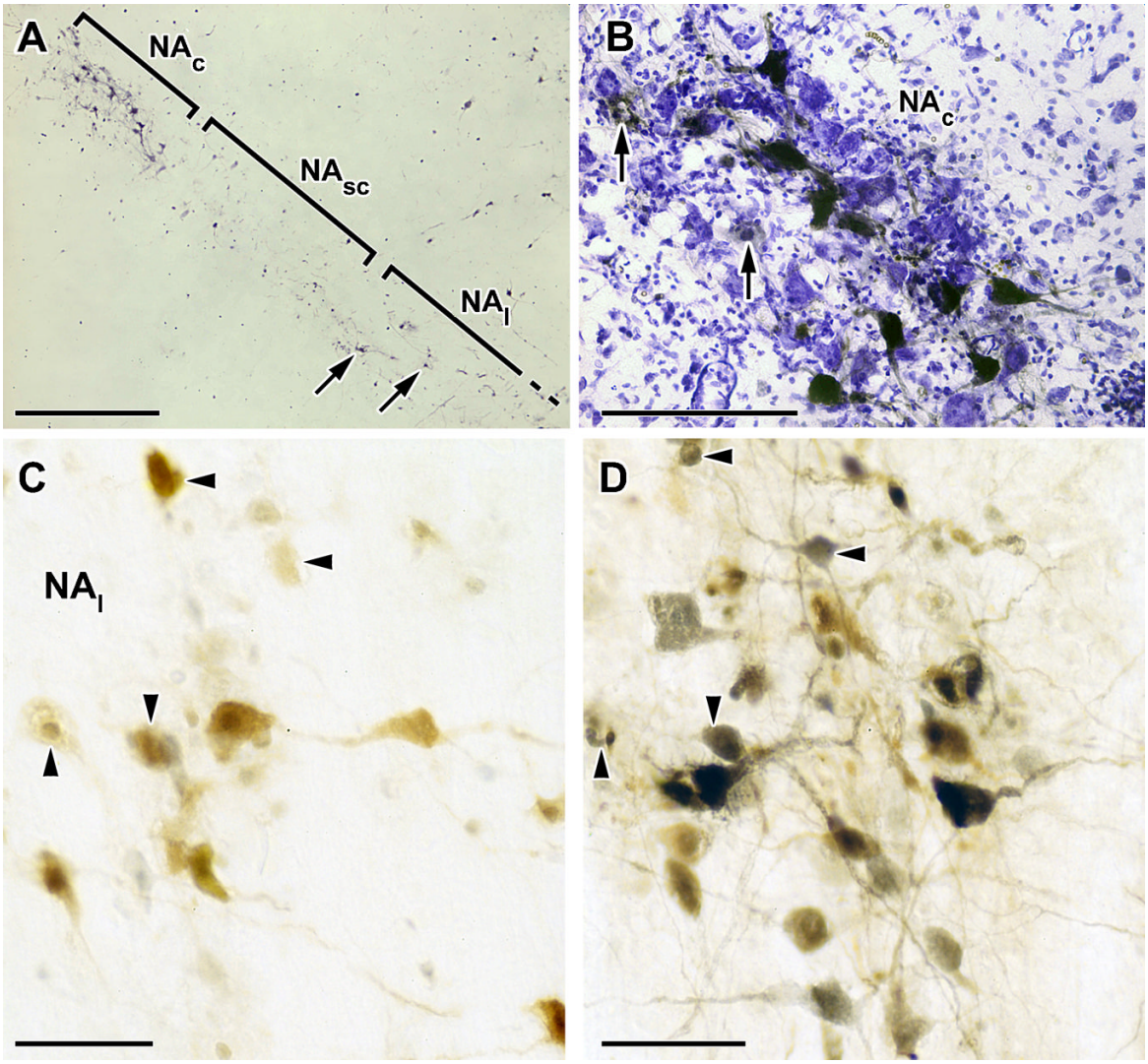

Figure 2.

Pseudorabies infection in the nucleus ambiguus.

A. Horizontal section, 50 μM thick, through the rat medulla showing immunostained PRV-GFP infected neurons in both the compact (NA_c) and loose (NA_l) portions of the nucleus ambiguus at four days after inoculation of the TA. Note the small number of NA_l neurons (arrows) and infection of the compact portion without infection of the intervening semi-compact portion. Scale bar: 1mm.

B. High power micrograph of the NA_c in a cresyl violet counterstained horizontal section showing (black) GFP-immunostained neurons typical of those consistently seen in this restricted portion of the compact NA four days after PRV-GFP inoculation of the TA. Note too the extensive gliosis and the ghost-like appearance of infected cells engulfed in glia (arrows). Scale bar: 100μM.

C. High power micrograph of a 50 μM thick section showing (brown) LacZ-immunostained neurons in the loose part of the NA following inoculation of PRV-LacZ into the posterior cricoarytenoid muscle (PCA). Scale bar: 50μM.

D. High power micrograph of the adjacent section to that shown in panel E but immunostained for both LacZ (brown) and GFP (black). PRV-GFP was injected at the same time into the TA as PRV-LacZ was injected into the PCA. Large motor neurons appear to be single-labeled but

some smaller neurons (arrowheads in this and panel E) appear immunoreactive for both viruses and appear in both sections. Scale bar: 50μM.

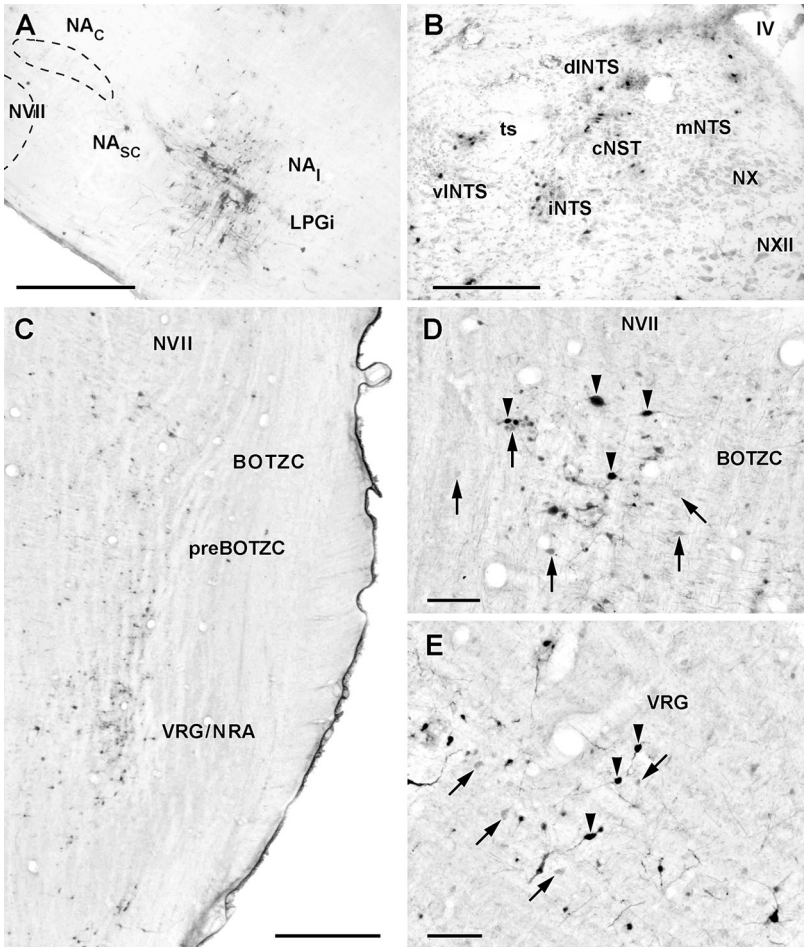

Figure 3.

Pattern of infection in the ventral and dorsal medulla four days after inoculation of PRV-GFP into the TA muscle.

A. Sagittal 50μM thick section through the rat medulla showing PRV-infected neurons in the loose NA and subjacent lateral paragigantocellularis nucleus (LPGi). Scale bar: 1mm

B. Coronal 50μM thick section (counterstained with cresyl violet) through the dorsal medulla showing PRV-infected neurons (black dots) in the central (cNTS) and intermediate (iNTS) divisions of the nucleus tractus solitarii. Scale bar:200μM.

C. Horizontal 50μM thick section through the ventral medulla showing PRV-infected neurons in the Bötzinger complex (BOTZC) just caudal to the facial nucleus (NVII) and ventral respiratory group/nucleus retroambigualis (VRG/NRA). Note the lack of infected neurons in the pre- Bötzinger complex (preBOTZC). Scale bar 1mm.

D. High power micrograph of PRV-infected neurons (arrowheads) in the Bötzinger complex. This section was also immunostained with an antibody to parvalbumin (PVAB) and numerous PVAB+ve neurons (arrows) can be seen intermingled with PRV-immunostained neurons. Scale bar: 100μM.

E. Similar section to that shown in panel D except showing PRV-infected neurons (arrowheads) interspersed with PVAB+ve neurons (arrows) in the ventral respiratory group. Scale bar: 100μM.

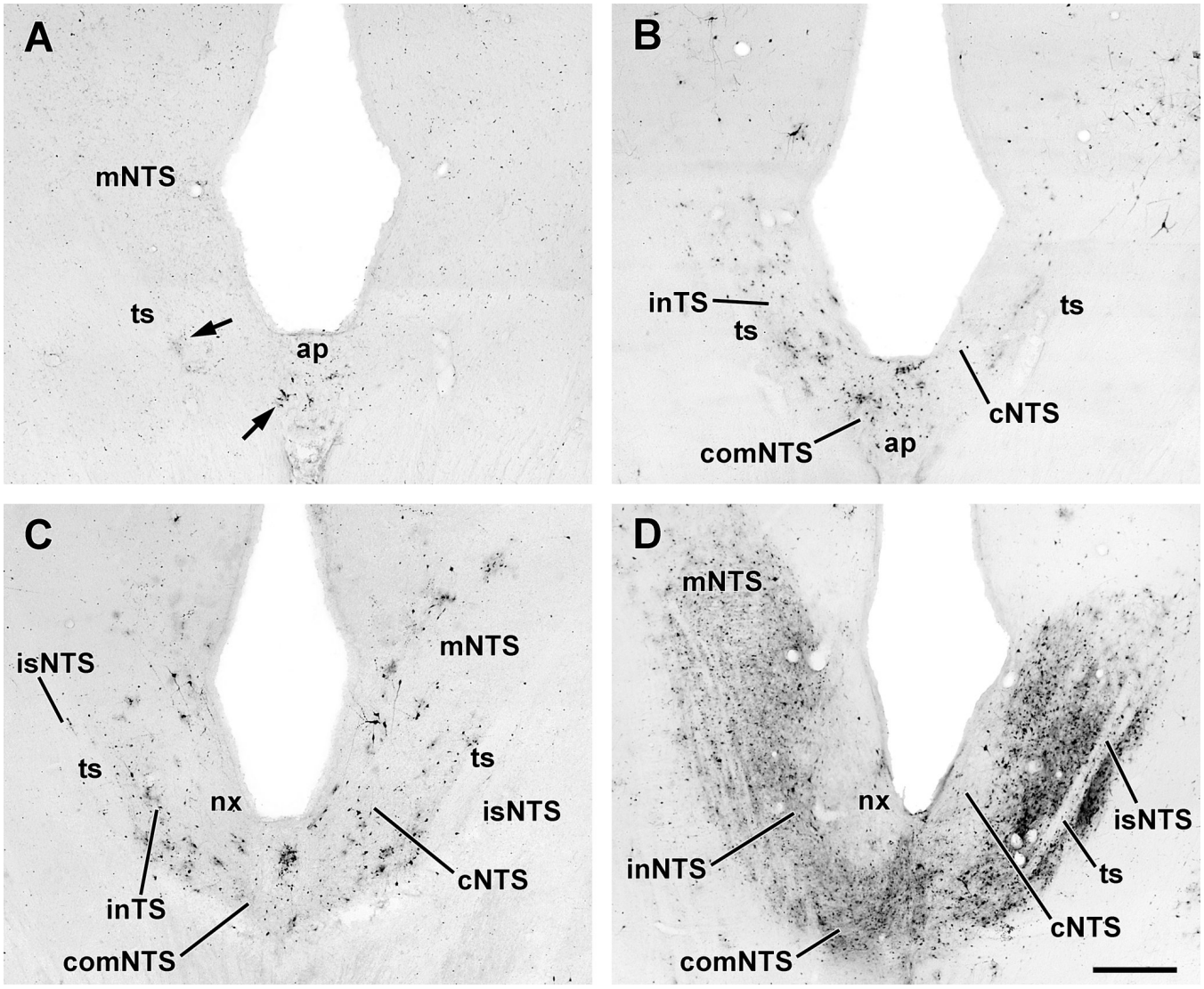

Figure 4.

Progression of infection in the nucleus tractus solitarii (NTS) following inoculation of PRV-GFP into the TA muscle. The sections shown in each panel are from approximately the same horizontal plane and show ipsilateral (left) and contralateral NTS.

A. Early 4 day; Note the early infection of neurons in the intermediate and central divisions (arrowheads). B. Late 4 day (sympathectomized). C. Early 5 day (sympathectomized). D. Late 5 day. Scale bar: 500μM.

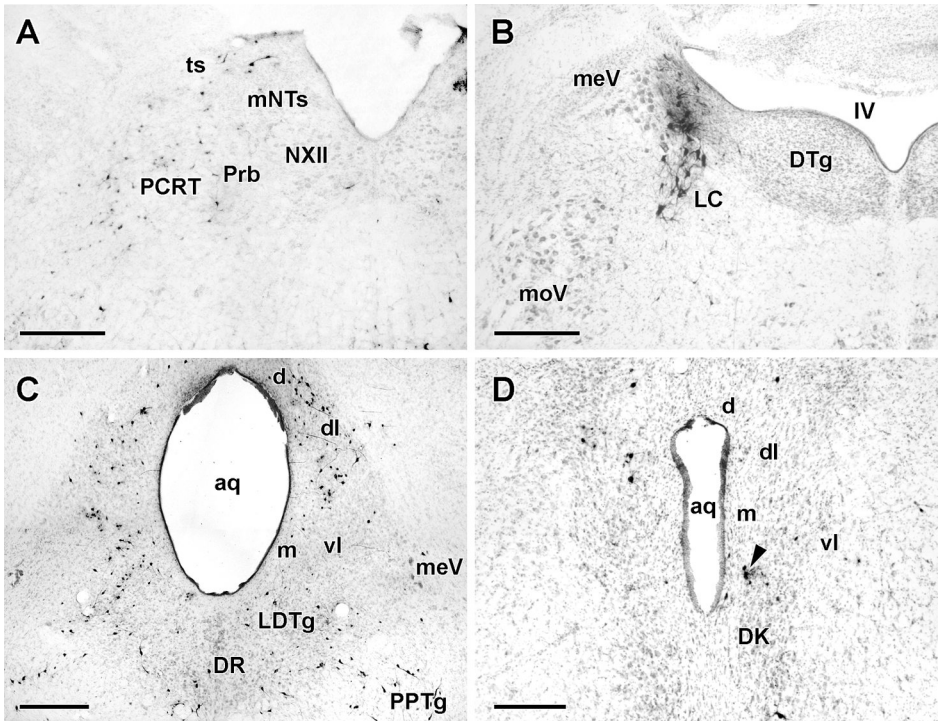

Figure 5.

Typical pattern of PRV infection in the medulla, pons and midbrain of cases sacrificed 5 days after inoculation of PRV-GFP into the TA muscle. The sections in panels A and B were from animals exhibiting the late day 4 pattern whereas those in panels C and D were from an animal with an early 5 day pattern of infection.

A. Coronal section (counterstained with cresyl violet) through the dorsal medulla showing infected neurons (black dots) in the ipsilateral rostral NTS (mNTS), parvocellular reticular formation (PCRT) and Probst's nucleus (Prb) just lateral to the hypoglossal nucleus (NXII).

B. Counterstained coronal section through the pontine tegmentum showing infection of the ipsilateral locus ceruleus (LC). In this case, neither the mesencephalic trigeminal nucleus (meV) nor the dorsal tegmental nucleus (DTg) contained infected neurons though these structures were typically infected in 5 day patterns. Scale bar: 200μM

C and D. Counterstained 50μM thick coronal sections through the caudal (C) and rostral (D) periaqueductal gray (PAG). In C, infection of neurons in the dorsal (d), dorsolateral (dl) and dorsal part of the ventrolateral (vl) divisions is present bilaterally while infection of the ventral part of vlPAG is present ipsilaterally. Note the infection of a band of neurons extending from the laterodorsal tegmental nucleus (LDtg) to the pedunculopontine tegmentum (PPTg). In sections additionally stained with an antibody to choline acetyltransferase, none of the neurons in this band were double labeled. In D, infection is fairly restricted to the ipsilateral dorsolateral (dl) division of the PAG though a small cluster of cells (arrow), probably in the supraoculomotor central gray, is present just dorsal to the nucleus of Darkschewitsch (Dk) contralaterally. Scale bars: 200μM.

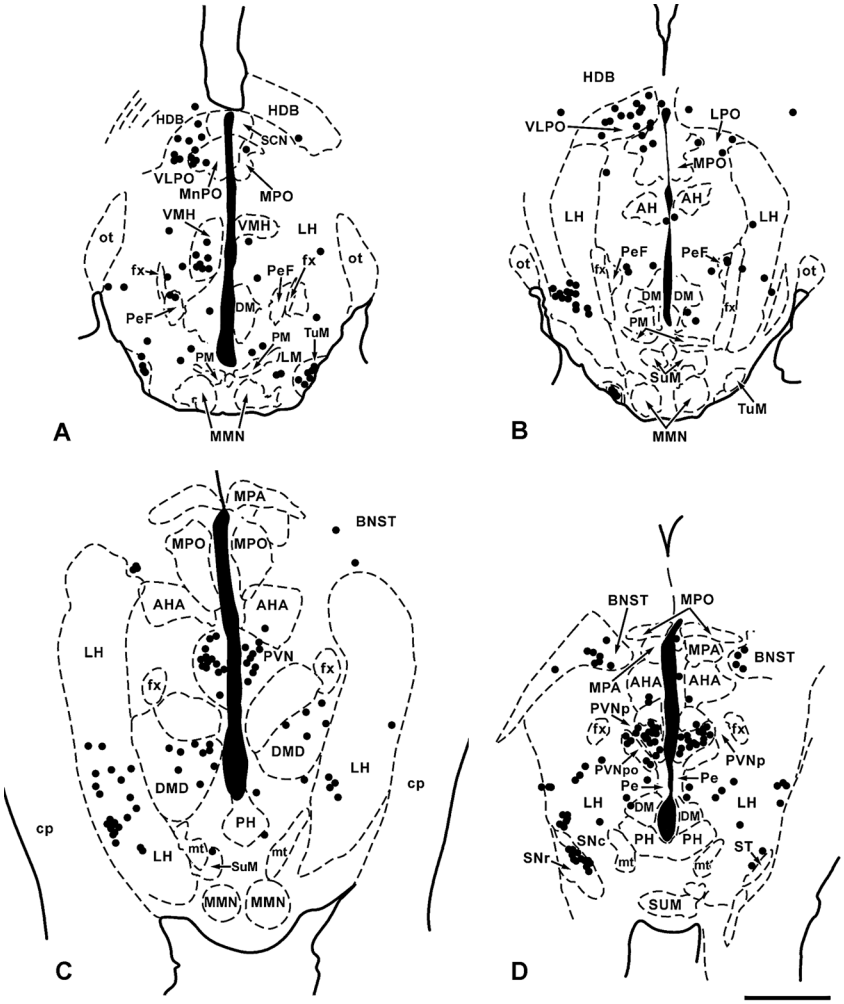

Figure 6.

A–D. Plots of the distribution of PRV-infected neurons (black dots) in four representative 50 μM thick horizontal sections through the hypothalamus from a sympathectomized animal receiving PRV-GFP into the TA muscle five days previously. Though sacrificed 5 days after inoculation this animal exhibited a typical late day 4 pattern of infection. Section A is the most ventral; section D the most dorsal and each black dot represents a single PRV-infected neuron. Scale bar:1mm

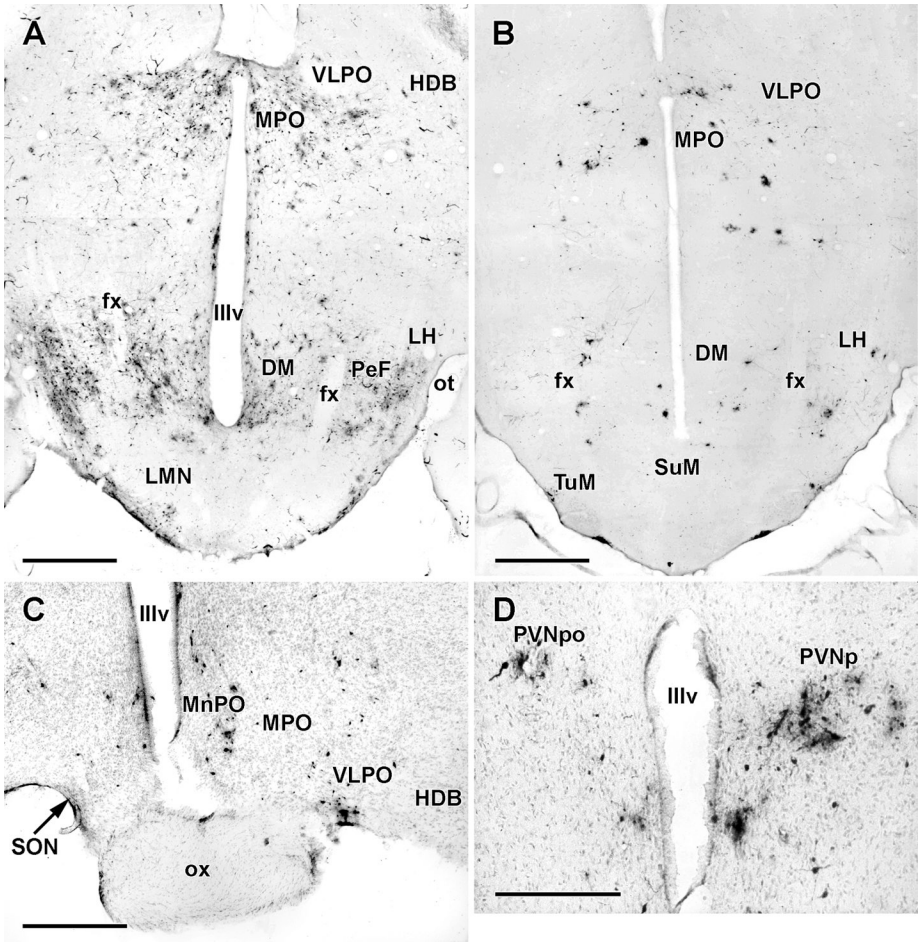

Figure 7.

PRV infection in the hypothalamus and differences between sympathectomized and non-sympathectomized animals.

A and B. Horizontal 50 μM thick sections through the ventral hypothalamus showing typical pattern of PRV infection in a non-sympathectomized animal with an early 5 day pattern (A) and a sympathectomized animal (B) with a late 4 day pattern. Note that despite a greater number of infected hypothalamic neurons in the intact animal (A) the overall distribution patterns are similar in terms of regional infection. The greatest difference appears to be in the almost complete disappearance of infection in the perifornical region (PeF) in the sympathectomized animal. Scale bar:1mm

C. Counterstained coronal section through the rostral hypothalamus from a sympathectomized animal sacrificed 5 days after PRV inoculation of the TA. Note the presence of infected neurons in the ipsilateral median (MnPO), medial (MPO) and ventrolateral (VLPO) preoptic areas. Scale bar: 500μM.

D. Counterstained coronal section through the hypothalamic paraventricular nucleus showing PRV-infected neurons in the parvocellular (PVNpo) division ipsilaterally and the posterior division contralaterally. This section (from the same animal shown in panel D) was cut asymmetrically and both divisions of the PVN were, in fact, infected bilaterally. Scale bar: 500μM

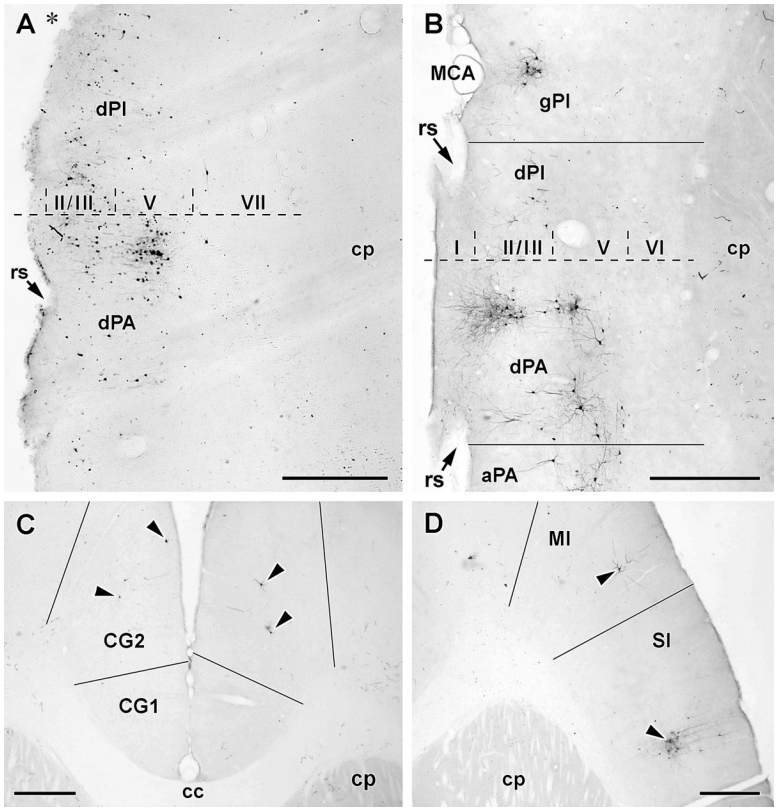

Figure 8.

Cortical pattern of infection following PRV inoculation of the TA. The black bars in panels B through D indicate the position of cortical boundaries determined from adjacent sections counterstained with cresyl violet. Scale bar in all panels: 500μM

A. Horizontal 50μM thick section through the rostral half of the cerebral cortex ipsilateral to the inoculated muscle. The animal from which this section was taken had been sympathectomized and sacrificed 4 days after inoculation. The dotted line marks the position of bregma as estimated from the anterior edge of the anterior commissure; Roman numerals indicate cortical laminae and the asterisk marks the position of the groove made by the middle cerebral artery (MCA). Note the infected neurons are concentrated in layer V of the dysgranular parietal insular cortex (dPA) at around the level of bregma.

B. Horizontal 50μM thick section through the rostral half of the cerebral cortex ipsilateral to the inoculated muscle, in this case from a sympathectomized animal sacrificed 5 days after PRV inoculation. Note the clustering of infected neurons in layers II/III and V in dPA around bregma but the expansion of infection to layers II/III of the granular posterior insular cortex (gPI) and layers II/III and V of the agranular PA (aPA).

C. Horizontal 50μM thick section through the medial prefrontal cortex either side of the midline. This section is approximately at the level where the genu of the corpus callosum (cc) reaches its most anterior extent. Note the presence of infected neurons in layer V of the cingulate area 2 (CG2) bilaterally. This section was from a sympathectomized animal sacrificed 5 days after PRV inoculation.

D. Horizontal 50μM thick section through the rostral frontal cortex *contralateral* to the inoculated muscle. This (sympathectomized) animal showed a typical early 5 day pattern of PRV infection. Note the clusters of infected neurons in motor (M1) and sensory (S1) cortices.

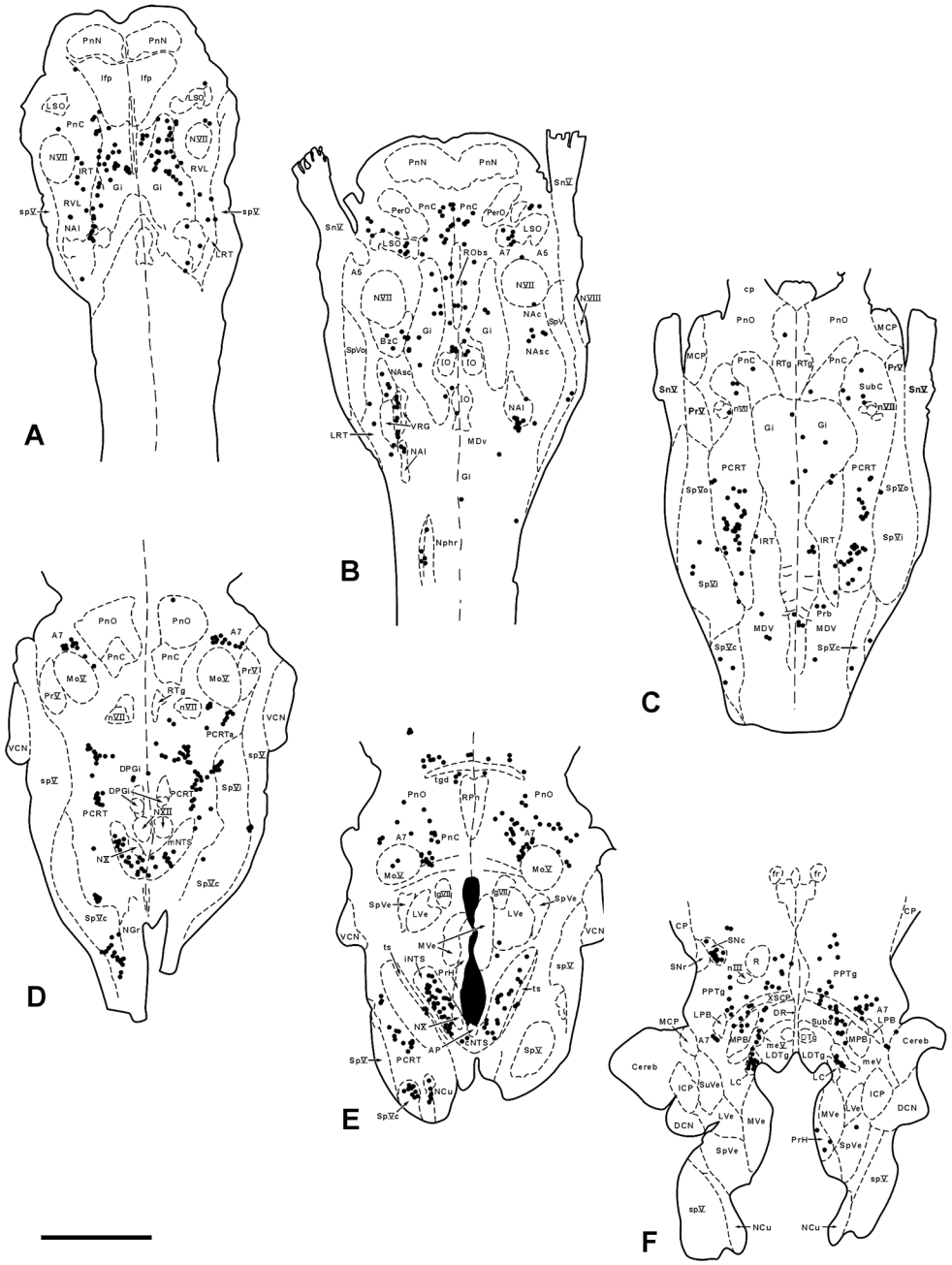

Figure 9.

Plots of infected neurons (black dots) in six representative 50μM thick horizontal sections through the pons and medulla from a sympathectomized animal sacrificed 5 days after inoculation of PRV into the TA. These plots show the typical early 5 day pattern. Section A is the most ventral and section F the most dorsal. Note the absence of infected neurons in the rostral ventrolateral medulla (RVL), A5 and area postrema (AP); these areas were almost always infected in non-sympathectomized animals. Scale bar: 2 mm

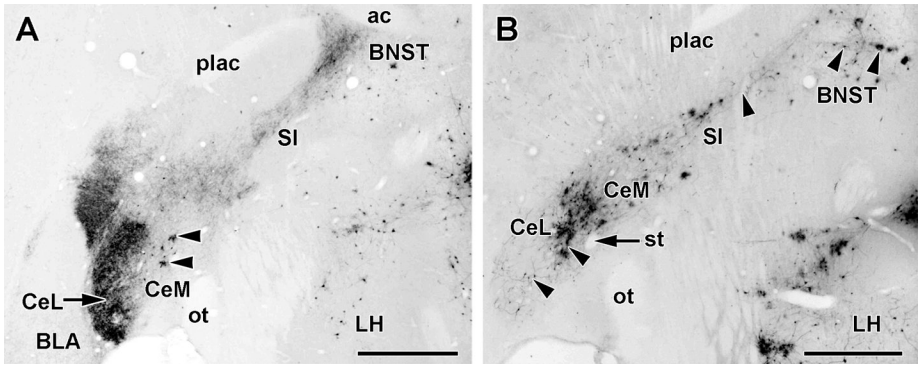

Figure 10.

PRV infection of the extended amygdala following inoculation of the TA muscle. Both panels show 50μM thick horizontal sections cut at the same dorso-ventral level from sympathectomized animals sacrificed at 4 (panel A) and 5 (panel B) days after TA inoculation. Scale bars: 1mm

A. In the typical late 4 day pattern of PRV infection, infected neurons (arrowheads) are virtually confined to the medial central nucleus (CeM). This section has been additionally stained using an antibody to CGRP which is heavily distributed in the lateral divisions of the central nucleus (CeL) and bed nucleus of the stria terminalis (BNST).

B. In the typical early 5 day pattern, PRV infected neurons (arrowheads) are now present in both CeM and CeL, the substantia innominata (SI) and the BNST.

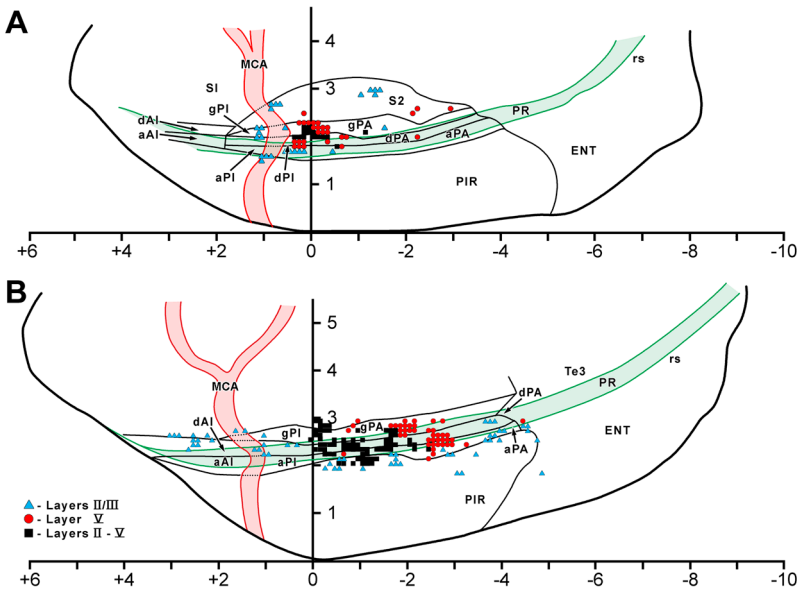

Figure 11.

Distribution plots of PRV infected cortical neurons projected onto the ipsilateral lateral cortical surface. These plots, and the positions of cortical boundaries, the middle cerebral artery and the rhinal sulcus were reconstructed from serial 50μM thick horizontal sections from sympathectomized animals. Alternate sections were counterstained with cresyl violet. Each point on the projection represents the laminar pattern of infection in a 100μM wide strip running perpendicular to the cortical surface; each point thus may represent more than one infected neuron. Color coding is used to identify which lamina(e) contain infected neurons. The scales are divided by 1 millimeter divisions and zero represents the position of bregma as determined from the position of anterior border of the anterior commissure.

A. Typical late 4 day pattern of cortical infection. Note the concentration of infected neurons in layer V of the dysgranular (dPA) and granular (gPA) around bregma.

B. Typical early 5 day pattern of cortical infection showing expansion over the 4 day pattern. Infection is present in all layers of gPA and dPA around bregma and there is infection now in layers II/III of agranular parietal (aPA), dysgranular anterior (dAI) and posterior (dPI) insular cortices as would be predicted by transneuronal infection through corticocortical connections. Note too the presence of a cluster of infected neurons in layer V of the dPA and aPA at around 2 millimeters behind bregma.

TABLE 1

Transneuronal Spread of PRV after Inoculation into the Thyroarytenoid Muscle

Postinoculation survival times				
≤ 3 day (n=4)	**Early 4 day (n=5) As previous, plus**	**Late 4 day (n=9) As previous, plus**	**Early 5 day (n=5) As previous, plus**	**Late 5 day (n=2)[2] As previous, plus**
N. ambiguus (loose)	N. ambiguus (compact)	N. ambiguus (compact) (X)	Phrenic n.	Prelimbic cortex (X)
Central NTS	Ventral respiratory group	N. ambiguous semicompact) (X)	N. cuneatus	M1 (X)
	Parvocellular reticular formation, (PCRT)	N. ambiguus (loose)	Commissural, interstitial and rostral NTS	
	N. gigantocellularis (X)[1]	Spinal n. of V	N. Pontis caudalis (X)	S1 (X)
	Probst's n.	Intermediate and medial NTS	Pedunculopontine tegmentum	
	Botzinger complex	PCRT (X)	Dorsal PAG	Subiculum (1/2)
	[Area postrema]	Intermediate reticular formation	Median preoptic area (X)	Hippocampus
	A7/subceruleus	Lateral para-gigantocellularis	Tuberomammillary n. (X)	Perirhinal cortex (X)
	[dorsolateral part of ventrolateral PAG]	Ventrolateral PAG (X)	Ventromedial hypothalamic n.	Entorhinal cortex (X)
	Dorsal raphe	Laterodorsal tegmental n.	Periventricular n.	
	[Perifornical area of hypothalamus] (X)	Locus ceruleus (X)	[Subfornical organ]	
		Mesencephalic V (X)	Dorsomedial hypothalamus (X)	
		Substantia nigra, pars reticulata	[Lateral septum]	
		Paraventricular n. of hypothalamus (X)	Medial Ce (X)	
		Medial preoptic area (X)	Lateral Ce (CeL)	
		Ventrolateral preoptic area (X)	Substantia innominata	
		Lateral hypothalamus (X)	Bed nucleus of stria terminalis	
		[Posterior hypothalamus]	Basolateral n. of amygdala (parvocellular)	
		Medial central n. of Amygdala (CeM)	Granular posterior insular cortex	
		Granular and dysgranular parietal insular cortex	Dysgranular parietal insular cortex (X)	
			Agranular parietal insular cortex	
		[Infralimbic cortex]	Dysgranular anterior insular cortex (X)	
		Entorhinal cortex	S2	
			M1 (XO)	
			CG2 (X)	

[1] X indicates infected cells were found bilaterally; XO indicates infected cells were found contralaterally only. All other sites are ipsilateral to the inoculated muscle.

[2] Viral clearance from pontomedullary structures is not indicated though both cases exhibited this in the nucleus ambiguus, NTS, and parvocellular reticular formation.

Table 2

Numbers of infected cell/cell fragments in the ipsilateral (i) and contralateral (c) NA and NTS subdivisions after inoculation of GFP-PRV into the thyroarytenoid muscle

	Case*		NA**				NTS***				AP
			l	*sc*	*c*	*m*	*c*	*is*	*i*	*com*	
Early 4 Day	1	*i*	15	0	5	1	1	0	0	0	0
		c	0	0	0	0		0	0	0	-
	2(s)	*i*	14	2	2	2	1	0	3	0	3
		c	0	0	0	1	1	0	1	0	-
	3(s)	*i*	10	0	0	2	0	0	12	3	2
		c	0	0	0	2	0	0	3	0	-
	4	*i*	2	0	0	2	0	0	0	0	0
		c	2	0	0	0	0	0	0	0	0
Late 4 Day	1	*i*	36	2	40	18	2	16	24	5	0
		c	9	0	12	7	2	0	9	0	-
	2	*i*	26	0	46	19	6	0	21	11	9
		c	1	0	1	0	3	0	12	7	-
	3(s)	*i*	40	13	62	17	9	14	66	7	0
		c	12	17	30	8	2	10	16	2	-
	4(s)	*i*	43	16	63	4	5	4	16	11	0
		c	36	2	41	6	3	0	5	2	-
Early 5 Day	1(s)	*i*	16	10	48	38	10	19	71	8	21
		c	38	4	52	24	13	9	27	12	-
	2	*i*	15	12	72	44	19	10	89	17	66
		c	18	3	24	21	17	0	59	13	-
	3(s)	*i*	16	10	52	23	18	12	71	8	7
		c	9	0	11	34	23	18	76	5	-
	4	*i*	39	10	46	13	1	2	25	8	8
		c	36	6	42	81	3	34	53	19	-
Late 5 Day	1(s)	*i*	24	4	46	11	5	5	46	46	0
		c	16	12	68	136	17	108	119	54	-

Case*		NA**				NTS***				AP
		l	*sc*	*c*	*m*	*c*	*is*	*i*	*com*	
2	*i*	17	5	34	66	19	17	78	26	17
	c	44	5	23	93	7	0	56	34	-
SLN 1	*i*	9	11	50	14	4	2	25	5	14
Transection	*c*	5	3	41	9	5	0	21	2	-
2	*i*	16	0	23	4	0	0	17	7	16
	c	4	0	7	0	0	20	15	2	-
RLN 1	*i*	0	0	0	0	0	0	0	0	12
Transection	*c*	7	0	39	12	0	2	1	0	-
2	*i*	0	0	0	0	0	0	0	0	0
	c	0	0	0	0	0	0	7	0	-
3	*i*	0	0	0	3	9	5	17	8	0
	c	0	0	0	12	0	5	10	7	-
Vagus 1	*i*	0	0	0	0	0	0	1	0	2
Transection	*c*	0	0	0	0	0	0	0	0	-
2	*i*	0	0	0	5	0	0	0	9	17
	c	2	0	0	9	0	0	0	12	-
3	*i*	0	0	0	0	0	0	0	3	9
	c	0	0	0	2	0	0	0	1	-

* Time points in experimental animals indicate pattern of labeling found, not necessarily the time animal was sacrificed post-inoculation. (s) indicates animals were sympathectomized.

** Numbers indicate the total number of infected cells in each subdivision of the NA estimated by counting only one fragment from each infected cell.

*** Numbers indicate the number of infected cell fragments greater than 10μM in diameter found in each subdivision on a single horizontal section through the dorsal-ventral midpoint of the NTS.